UNIVERSIDADE FEDERAL DE VIÇOSA

LUÍS FERNANDO JANUÁRIO ALMEIDA

PLANT MATERIAL CONTROLS SOIL ORGANIC MATTER FORMATION AND THE MAGNITUDE OF PRIMING EFFECT

VIÇOSA – MINAS GERAIS
2020

LUÍS FERNANDO JANUÁRIO ALMEIDA

PLANT MATERIAL CONTROLS SOIL ORGANIC MATTER FORMATION AND THE MAGNITUDE OF PRIMING EFFECT

Tese apresentada à Universidade Federal de Viçosa, como parte das exigências do Programa de Pós-Graduação em Solos e Nutrição de Plantas, para obtenção do título de *Doctor Scientiae*.

Orientador: Ivo Ribeiro da Silva

Coorientadores: Leonardus Vergutz
Samuel V. Valadares

VIÇOSA – MINAS GERAIS
2020

Ficha catalográfica elaborada pela Biblioteca Central da Universidade Federal de Viçosa - Campus Viçosa

T
A447p
2020

Januário Almeida, Luís Fernando, 1990-
Plant material controls soil organic matter formation and the magnitude of priming effect [recurso eletrônico] / Luís Fernando Januário Almeida. – Viçosa, MG, 2020.
84 f.: il. (algumas color.).

Orientador: Ivo Ribeiro da Silva.
Tese (doutorado) - Universidade Federal de Viçosa.
Inclui bibliografia.

1. Química do solo. 2. Humus. 3. Respiração microbiana. 4. Análise espectral. I. Universidade Federal de Viçosa. Departamento de Solos. Programa de Pós-Graduação em Solos e Nutrição de Plantas. II. Título.

CDD 22. ed. 631.417

Bibliotecário(a) responsável: Renata de Fatima Alves CRB6/2578

LUÍS FERNANDO JANUÁRIO ALMEIDA

PLANT MATERIAL CONTROLS SOIL ORGANIC MATTER FORMATION AND THE MAGNITUDE OF PRIMING EFFECT

Tese apresentada à Universidade Federal de Viçosa, como parte das exigências do Programa de Pós-Graduação em Solos e Nutrição de Plantas, para obtenção do título de *Doctor Scientiae.*

APROVADA: 31 de março de 2020.

Assentimento:

Luís Fernando Januário Almeida
Autor

Ivo Ribeiro da Silva
Orientador

AGRADECIMENTOS

Em primeiro lugar, a Deus, pelo dom da vida.

À Universidade Federal de Viçosa e ao Departamento de Solos, por possibilitar a realização deste curso de doutorado.

À *Technische Universität München* (TUM) e ao *Lehrstuhl für Bodenkunde*, pelo acolhimento durante o período de doutorado sanduíche e por possibilitar a realização de boa parte das análises do presente estudo.

À FAPEMIG, ao CNPq e ao Grupo NUTREE pelo auxílio financeiro, e em especial à CAPES pelo financiamento do período de estágio no exterior por meio do processo número 88881.189468/2018-01.

Ao Professor Ivo Ribeiro, pela amizade, orientação, incentivo e apoio desde a graduação.

Ao Dr. Ivan Francisco de Souza, pela amizade, constante orientação e contribuição para o presente trabalho com suas considerações curtas, francas e sinceras.

Ao Dr. Carsten Müller, pela amizade, orientação e suporte na condução das atividades de pesquisa durante o período de intercâmbio na TUM.

Aos Professores Leonardus Vergutz e Samuel Vasconcelos Valadares, pela colaboração na realização deste trabalho.

Aos demais Professores do Departamento de Solos, por contribuírem para minha formação, em especial João Carlos Ker, Jaime Mello, Júlio César Lima Neves, Nairam Félix de Barros, Emanuelle Soares e Edson Mattiello.

Aos técnicos do Laboratório de Isótopos Estáveis (LIE) João Milagres e Humberto, pela constante ajuda e pela importante contribuição para a realização deste trabalho.

Aos estagiários pelas contribuições na execução dos experimentos.

Aos amigos e colegas da Pós-graduação, em especial Bernardo, Daniela, Gustavo, Ana, Pedro.

Aos amigos e colegas da TUM, Luís Colocho, Noelia, Thiago Inagaki, Chris, Franzi(s), Evelin, Julien, Yaser, Tianyi e Steffen.

Aos membros da banca Professor Teógenes Senna de Oliveira, Professor Maurício Dutra Costa, Professor Samuel Vasconcelos Valadares e Dr. Guilherme Luiz de Jesus pela disponibilidade em participar da banca de defesa e pelas sugestões de melhoria no presente trabalho.

Aos meus queridos pais, Francisco e Maria da Conceição, meus irmãos, Sidnei, Silvério e Bruno pelo constante apoio e incentivo.

À Patrícia pelo companheirismo e compreensão em todos os momentos.

Aos meus amigos de longa data pelo incentivo constante aos estudos, em especial Marx, Robertinho, Viviane e Gustavão.

BIOGRAFIA

LUÍS FERNANDO JANUÁRIO ALMEIDA, filho de Francisco Tibúrcio de Almeida e Maria da Conceição Januário Almeida, nasceu em 24 de março de 1990, em Santo Antônio do Grama – MG.

Em dezembro de 2007, concluiu o ensino médio na Escola Estadual Effie Rolfs, em Viçosa – MG.

Em março de 2008, iniciou o curso de graduação em Agronomia pela Universidade Federal de Viçosa, concluindo-o em março de 2014.

Entre agosto de 2010 e março de 2011, foi bolsista do programa CAPES/FIPSE na modalidade “graduação sanduíche”, na Florida Agricultural and Mechanical University (FAMU), sob orientação do Professor Dr. Clifford Louime e da Pesquisadora Associada Dr. Amita Jain.

Em março de 2014, iniciou o curso de Mestrado em Solos e Nutrição de Plantas na Universidade Federal de Viçosa sob orientação do Professor Ivo Ribeiro da Silva, concluindo-o em fevereiro de 2014.

Em março de 2016, ingressou no Programa de Pós-Graduação em Solos e Nutrição de Plantas na Universidade Federal de Viçosa, em nível de Doutorado, sob orientação do Professor Ivo Ribeiro da Silva, submetendo-se à defesa de tese em março de 2020.

Entre agosto de 2018 e junho de 2019, foi bolsista do programa CAPES/PDSE na modalidade “doutorado sanduíche”, na *Technische Universität München* (TUM), sob orientação do Dr. Carsten Müller.

.

“The mind that opens up to a new idea never returns to its original size". (Albert Einstein)

RESUMO

ALMEIDA, Luís Fernando Januário, D.Sc., Universidade Federal de Viçosa, março de 2020. **O material vegetal controla a formação da matéria orgânica do solo e a magnitude do efeito priming.** Orientador: Ivo Ribeiro da Silva. Coorientadores: Leonardus Vergutz e Samuel Vasconcelos Valadares.

A matéria orgânica do solo (MOS) tem capacidade para armazenar grandes quantidades de carbono (C). Nesse contexto, a MOS é um dreno potencial para o C atmosférico e uma alternativa para a mitigação do aquecimento global. Embora a MOS seja amplamente investigada, os processos que governam sua formação e retenção nos solos não são totalmente compreendidos. Assim, objetivou-se no presente estudo compreender como a composição química do *litter* de planta governa a formação da MOS nova e a mineralização da MOS "nativa". A pesquisa foi dividida em duas partes que originaram dois capítulos: I) *Quantitative parametrization of molecular diversity and microbial respiration of biochemical fractions of eucalypt plant tissues***;** and II) *Forest litter constraints on the pathways controlling soil organic matter formation*. Para o capítulo I, fracionamos os componentes de plantas de eucalipto por meio de análise proximal (AP), a qual tem sido amplamente utilizada para determinar a composição química do *litter* em estudos de decomposição. As frações obtidas tiveram sua composição bioquímica caracterizada por espectroscopia de RMN de ^{13}C e termoquimólise acoplada a cromatografia gasosa e espectrometria de massas. Após essa caracterização, órgãos artificiais de plantas foram "reconstruídos" e incubados em amostras de solo por 200 dias sob condições controladas. Nossos resultados demonstraram que a composição química governa a respiração do material vegetal nos estágios iniciais da decomposição. Por outro lado, nos estágios finais da decomposição, as propriedades do substrato não tiveram influência significativa na liberação de $C\text{-}CO_2$. Para o capítulo II, incubamos amostras de solo com diferentes órgãos de plantas de eucalipto por 200 dias. Esses órgãos representavam frações do *litter* de florestas de composição química distinta e de diferentes localizações usuais de entrada no solo (acima e abaixo do solo). Para cada tratamento, determinamos a quantidade de C derivado do *litter* incorporada em diferentes frações da MOS, assim como o efeito *priming* causado pelo aporte do *litter*. Nossos resultados indicaram que o *litter* de parte aérea foi respirado em taxas mais elevadas, mas causou uma menor

degradação da MOS nativa comparado com o *litter* de raiz. Além disso, o *litter* de parte aérea contribuiu para ganhos líquidos na POM e na MAOM, enquanto o *litter* de raiz levou a ganhos líquidos apenas na POM. De modo geral, a formação de MOS via incorporação microbiana de *litter* de parte aérea por meio de vias *in vivo* parece ser mais eficiente e causar menos degradação de MAOM “nativa” do que raízes.

Palavras-chave: Bioquímica do substrato. Respiração microbiana. Rota in vivo. Rota ex vivo. Efeito priming. Espectroscopia ^{13}C-CP/MAS-NMR. Litter de parte aérea. Litter de raiz. Matéria orgânica particulada. Matéria orgânica associada aos minerais.

ABSTRACT

ALMEIDA, Luís Fernando Januário, D.Sc., Universidade Federal de Viçosa, March, 2020. **Plant material controls soil organic matter formation and the magnitude of priming effect.** Adviser: Ivo Ribeiro da Silva. Co-advisers: Leonardus Vergutz and Samuel Vasconcelos Valadares.

Soil organic matter (SOM) has the capacity to store large amounts of carbon (C). In this context, SOM is a potential sink of atmospheric C and an alternative for global warming mitigation. Although SOM is widely investigated, the processes governing its formation and retention in soils are not completely understood. Thus, we aimed in the present study to understand how the chemical composition of plant litter drives the formation of new SOM and the mineralization of "native" SOM. The research was divided in two parts that originated two chapters: I) *Quantitative parametrization of molecular diversity and microbial respiration of biochemical fractions of eucalypt plant tissues***;** and II) *Forest litter constraints on the pathways controlling soil organic matter formation*. For the chapter I we fractionated eucalypt plant components through proximate analysis (PA), which has been widely used to determine litter chemistry in decomposition studies. The fractions obtained had their biochemical composition characterized by ^{13}C-NMR spectroscopy and thermochemolysis coupled to gas chromatography-mass spectrometry. After this characterization, artificial plant organs were "reconstructed" and incubated in soil samples for 200-days under controlled conditions. Our results showed that the chemical composition of substrate drives the respiration of plant material at the early stages of decomposition. Conversely, at the late stages of decomposition substrate properties had no significant influence on C-CO_2 release. For the chapter II we incubated soil samples with different eucalypt plant organs for 200 days. These plant organs represented forest litter fractions with distinct chemical composition and usual input location in soil (above and belowground). For each treatment, we determined the amount of litter-derived C incorporated into different SOM fractions as well as the priming effect caused by the fresh litter amendments. Our results indicate that the aboveground litter were respired at higher rates but caused less native SOM degradation as compared to root litter. Additionally, aboveground litter contributed to net gains in both POM and MAOM, while root litter only led to net gains in POM. Generally, SOM formation via microbial incorporation of

aboveground litter through *in vivo* pathways appears to be more efficient and causes less degradation of “native” MAOM than roots.

Keywords: Substrate biochemistry. Microbial respiration. In vivo pathway. Ex vivo pathway. Priming effect. ^{13}C-CP/MAS-NMR spectroscopy. Aboveground litter. Root litter. Particulate organic matter. Mineral-associated organic matter.

SUMÁRIO

1. GENERAL INTRODUCTION

Forest soils contain approximately 75 % of global soil C stocks and has been considered as a potential sink for atmospheric C (LAL, 2005; SCHMIDT et al., 2011). However, the effective utilization of natural or managed forests for C sequestration is not trivial (JACKSON et al., 2017; LAJTHA et al., 2018). This is partially because the mechanisms governing litter decomposition, SOM formation and its retention in soil are not completely elucidated.

Chemical composition is regarded as the main controller of litter decomposition and, consequently, the SOM formation (COTRUFO et al., 2015). In addition to their distinct composition, plant materials that enter in the soil system are spatially constrained (e. g., above and belowground), what can also contribute to their incorporation into SOM. Currently, there is evidence that plant material is incorporated into SOM through two distinct pathways: i) *in vivo* turnover and ii) *ex vivo* modification (LIANG; SCHIMEL; JASTROW, 2017). In the first pathway the plant material is processed by soil microbes and afterwards transferred to SOM as microbial products. However, in the second pathway the plant material is not assimilated by the microorganisms, but instead broke down towards smaller subunits by microbial extracellular enzymes. Therefore, litter fractions considered labile are more likely to be converted in SOM through the *in vivo* turnover. Conversely, the *ex vivo* modification is apparently the prevailing pathway for SOM formation from plant components considered recalcitrant (ALMEIDA et al., 2018; COTRUFO et al., 2015; HADDIX; PAUL; COTRUFO, 2016). Nevertheless, the extent to which these SOM formation pathways are affected by litter chemical composition and its input location still remains unclear.

The SOM accrual depends on the positive balance between SOM formation from the vegetation inputs and the decomposition of native SOM (DAVIDSON; JANSSENS, 2006). Nevertheless, the SOM investigations mainly focus on litter decomposition and newly formed SOM, while less attention is given to “native” SOM mineralization as affected by the fresh litter inputs (priming effect). This process is complex and depends simultaneously on several factors, making the relationship between the chemical composition of plant litter inputs and the magnitude of the priming not straightforward (CHEN et al., 2014; FONTAINE; MARIOTTI; ABBADIE,

2003; KUZYAKOV; FRIEDEL; STAHR, 2000; LYU et al., 2019). Therefore, understanding the mechanisms that govern the priming effect caused by plant materials with distinct composition are necessary and to increase C sequestration in managed soils.

The main objective of the present study was to understand how the chemical composition of eucalypt litter drives the SOM formation as well as the mineralization of "native" SOM. To this end, the investigation was divided in two chapters: I) *Quantitative parametrization of molecular diversity and microbial respiration of biochemical fractions of eucalypt plant tissues***;** and II) *Forest litter constraints on the pathways controlling soil organic matter formation*. For the chapter I we fractionated the eucalypt plant components through proximate analysis (PA) based methods, which has been widely used to determine litter chemistry in decomposition studies. Additionally, we determined the molecular composition of eucalypt plant organs and their respective biochemical fractions obtained by ^{13}C-NMR spectroscopy and thermochemolysis coupled to gas chromatography-mass spectrometry. After this characterization, artificial plant organs were "reconstructed" and incubated in soil samples under controlled conditions for 200-days, during which we monitored the evolution of ^{13}C-CO_2 from the microcosms. This allowed us to determine the efficiency of PA-based methods in separate group of compounds with similar chemical properties, and determine which characteristics are useful to predict their behavior in soil. For the chapter II we incubated different eucalypt plant organs that represented litter fractions with distinct chemical composition. For each treatment we determined the litter-derived C incorporated into different SOM as well as priming effect caused by the fresh litter inputs. Thus, we could stablish the relationship between litter chemistry, its decomposition and SOM formation, as well as determine the magnitude of priming effect caused by plant materials with distinct composition.

2. CHAPTER I - QUANTITATIVE PARAMETRIZATION OF MOLECULAR DIVERSITY AND MICROBIAL RESPIRATION OF BIOCHEMICAL FRACTIONS OF EUCALYPT PLANT TISSUES

2.1. Abstract

Quantitative assessments on molecular diversity of plant litter fractions and its impact on microbial respiration remain scarce. To address this issue, we fractionated leaves, twigs, bark, wood, and root tissues of ^{13}C-enriched eucalypt seedlings into hot water extractables (HWE), total solvent extractables (TSE), a cellulosic fraction (CF), and the acid unhydrolyzable residue (AUR). These fractions were characterized using bulk chemistry, ^{13}C-NMR spectroscopy and thermochemolysis coupled to off-line gas chromatography-mass spectrometry. Afterwards, equal proportions of HWE, CF, TSE and AUR (25% each) were used to 'reconstruct' artificial plant organs and incubated into a Haplic Ferralsol for 200-days in laboratory/controlled conditions. Our results showed that over the first two days of incubation, the HWE fraction was the predominant ^{13}C-CO_2 source and substrate respiration was constrained by long C chains, H:C ratio, and carbonylic functional groups. Subsequently (3-45 days), the CF was respired at higher rates than HWE, with strong release of ^{13}C-CO_2 from carbohydrates and short C chains with high O:C ratio. Over the last 92-200 days of incubation, substrate properties had no significant influence on ^{13}C-CO_2 release. Overall, microbes respired much more on CF and HWE than TSE (lipid-rich) or AUR (lignin-rich). Although both fractions showed high proportions of mid (11-29 C atoms) and long C chains (>30 C atoms), AUR had a comparatively higher molecular diversity than TSE. Therefore, functional groups and the molecular weight of the constituents of biochemical fractions of eucalypt plant tissues provide a quantitative assessment of their molecular diversity. Otherwise, substrate selection and microbial respiration appear to be more sensitive to energetic constraints than intrinsic molecular diversity.

Keywords: Proximate analysis. ^{13}C. Substrate Biochemistry. ^{13}C-CP/MAS-NMR spectroscopy. Thermochemolysis. Microbial respiration.

2.2. Introduction

Over the last decades, there has been a substantial paradigm change about the role of substrate chemistry and microbial activity controlling the fate of plant litter in soils. On one hand, the very long-standing premise of substrate intrinsic 'recalcitrance' controlling soil organic matter (SOM) formation and persistence has been increasingly challenged (DUNGAIT et al., 2012; KLEBER, 2010; MARSCHNER et al., 2008; SCHMIDT et al., 2011). On the other hand, the role of the products of microbial metabolism as major building blocks driving SOM formation have been increasingly recognized (BRADFORD et al., 2013; COTRUFO et al., 2013; GRANDY; NEFF, 2008; KALLENBACH; FREY; GRANDY, 2016; LIANG; SCHIMEL; JASTROW, 2017). Recently, these two aspects have been merged into a new concept, according to which the influence of substrate molecular diversity on microbial metabolism is central for both plant litter and SOM dynamics (LEHMANN et al., 2020). However, quantitative parameters to express substrate molecular diversity remain elusive, partly due to the inherent heterogeneity of plant litter and/or technical limitations.

Beyond the total contents of C, N and other elements, proximate analyses have long been used to isolate specific fractions of plant litter (OSONO; TAKEDA; AZUMA, 2008; PRESTON; TROFYMOW, 2000; RYAN; MELILLO; RICCA, 1990; SJÖBERG et al., 2004). To some extent, these procedures can give a glimpse of litter molecular diversity. Usually, proximate analyses include a stepwise treatment of plant litter aiming to extract soluble materials either in water (polar substances) or organic solvents (non-polar substances), and structural components such as cellulose, hemicellulose and lignin (PRESTON; TROFYMOW, 2015). According to these authors, these fractions can be heterogeneous, and lignin is certainly the most problematic. Generally, lignin content in plant materials is usually inferred from the acid unhydrolyzable residue (AUR) obtained after removing soluble fractions (polar and non-polar) and treating the material remaining with H_2SO_4 (72%) under reflux (RYAN; MELILLO; RICCA, 1990). Hence, despite the undeniable usefulness of proximate analysis, the fractions obtained from such procedures require detailed characterization, especially the AUR obtained from non-woody materials (KÖGEL-KNABNER; RUMPEL, 2018; PRESTON; NAULT; TROFYMOW, 2009; ZECH et al., 1987). Given the overall complex mixture of plant litter or even its fractions obtained

via proximate analyses, a detailed characterization of these materials is an important step to achieve a quantitative parameterization of their molecular diversity.

Although there are several methods and techniques allowing the characterization of plant litter fractions, solid-state ^{13}C nuclear magnetic resonance (NMR) spectroscopy coupled to cross-polarization magic angle spinning (CPMAS) is among the most powerful (KÖGEL-KNABNER; RUMPEL, 2018; PRESTON; TROFYMOW, 2015). Generally, NMR-CPMAS probes the "chemical environment" around C atoms allowing the quantification of alkyl C, N-alkyl/methoxy C, O-alkyl C, aromatic C, and carbonylic C groups (NELSON; BALDOCK, 2005). These authors also developed a molecular mixing model according to which NMR data can be used to estimate the nominal oxidation state of C (NOSC) of the constituents of a given organic material. Nonetheless, NMR experiments do not offer any specific indications about the molecular weight of the constituents of plant litter fractions obtained in proximate analysis. To this end, these fractions can be further treated with tetramethylammonium hydroxide (TMAH) thermochemolysis and the molecular weight of its predominant constituents can be assessed by off-line gas chromatography (ALMEIDA et al., 2018; KLOTZBÜCHER et al., 2011). These aspects are important to determine the extent to which the fate of C in soils is impacted by the molecular diversity of plant litter fractions as inferred from their predominant C bonds and the size of the molecules in which these bonds occur.

In our study, we used proximate analysis to obtain hot water extractables, total solvent extractables, a cellulosic fraction and the acid unhydrolyzable residue from ^{13}C-labeled eucalypt seedlings. We characterized the biochemical fractions using NMR-CPMAS and the molecular mixing model to quantify the proportions of major functional groups, NOSC and elemental ratios (N:C, H:C and O:C ratios). Further, termochemolysis coupled to off-line gas chromatography and mass spectrometry (GC-MS) were used to quantify the molecular weight of the major compounds within each biochemical fraction. Subsequently, we used equal proportions of the biochemical fractions (25%) to 'reconstruct' artificial leaves, twigs, bark and roots. Hence, we could eliminate the influence of different proportions of each biochemical fraction that would occur in natural plant organs. As a result, we could determine the extent to which the respiration of one biochemical fraction can affect one another and the impact of specific functional groups and the size of C chains on microbial respiration. We used the

artificial plant organs to incubate soil samples of a Haplic Ferralsol for 200 days, during which we monitored the evolution of ^{13}C-CO_2 from the microcosms. The release of ^{13}C-CO_2 would provide the best estimate possible of the proportion of each substrate effectively taken up and metabolized by soil microbes.

2.3. Material and methods

2.3.1. Plant growth and isotopic labeling

For the present study, we grew clonal eucalypt clonal seedlings (hybrids of *Eucalyptus grandis* × *E. urophylla*) into a growth chamber (448.0 dm^3) under constant aeration. Inside the growth chamber, the seedlings were placed into polyethylene vessels (3.5 L capacity) and all nutrients were supplied via Clark nutrient solutions (CLARK, 1975). During the growth period, half of the plants were pulse-labeled with ^{13}C-CO_2 stable isotope, which was done by acidifying $Na_2{}^{13}CO_3$ with concentrated H_2SO_4. In order to achieve similar experimental conditions for unlabeled plants, half of the seedlings also were submitted to increased concentrations of CO_2 by acidifying $Na_2{}^{12}CO_3$ with concentrated H_2SO_4. After the labeling period (126 days), the plants were harvested and fractionated into leaves, twigs, bark, wood and roots. All plant organs were dried to constant weight under a forced-draft oven at 60 ℃, ground into a Wiley mill and stored for the chemical fractionation and subsequent analysis. Total C, N and ^{13}C content of the plant organs are given in Table 1.

Table 1. Mean and standard error for total carbon, nitrogen, C:N ratio, and isotopic data expressed in $\delta^{13}C_{\text{-PDB}}$ and ^{13}C-atom% of each plant organ (leaves, twigs, bark, wood, and roots) of eucalypt seedlings

Plant Organ	C, g kg^{-1}	N, g kg^{-1}	C:N	$\delta^{13}C_{\text{-PDB}}$	^{13}C-atom%
Leaves	440.9 ± 3.9	18.3 ± 1.0	24	425.1 ± 10.9	1.6 ± 0.0
Twigs	429.0 ± 10.4	7.6 ± 0.5	56	359.6 ± 31.9	1.5 ± 0.0
Bark	416.4 ± 1.7	5.2 ± 0.1	80	319.1 ± 16.7	1.4 ± 0.0
Wood	437.7 ± 7.4	2.0 ± 0.2	219	290.3 ± 14.0	1.4 ± 0.0
Roots	435.6 ± 16.2	10.4 ± 0.5	42	377.9 ± 35.1	1.5 ± 0.0

2.3.2. Isolation of the biochemical fractions of plant tissues

Subsamples of all plant organs (leaves, twigs, bark, wood and roots) were chemically fractioned into four operationally defined “biochemical fractions”, namely: hot water extractables (HWE), total solvent extractables (TSE), a cellulosic fraction (CF) and the acid unhydrolyzable residue (AUR). These fractions were obtained from the isotopically labeled and unlabeled plant material. Briefly, two g of each plant component (particle-size ≤ 0.425 mm) were extracted in Soxhlets with 150 mL of deionized water at 100 ℃ for 6 hours to obtain the HWE. Likewise, two g of the residue generated after the HWE extraction were Soxhlet-extracted with 150 mL of acetone at 56 ℃ for 6 hours to obtain the TSE. For the extraction of HWE and TSE, the temperatures indicated are the minimum values required to evaporate each solvent used, which subsequently condensates before interacting with the sample in Soxhlet. After the extraction, both HWE and TSE were freeze-dried and stored. The residue free of HWE and TSE was subsequently fractioned into the CF or AUR in separate procedures. Accordingly, the CF was obtained by treating one g of the residue with a mixture of ethanol and aqueous HNO_3 (65%, v/v) at a ratio of 4:1 at 85 ℃ for 1 h. This extraction was repeated four times and the residue generated was treated with an aqueous solution of KOH 25% (m/v) at 100℃ for 1 h. For the isolation of the AUR fraction, one g of the residue free of HWE and TSE was treated with 6 mL of aqueous H_2SO_4 (72%, v/v) at 30 ℃ and kept in water bath during 1 h. Subsequently, we added 140 mL of distilled water and the temperature was raised to 100 ℃ and kept constant during 4 h. Both CF and AUR were washed extensively with ultra-pure water, freeze-dried and stored.

2.3.3. Characterization of plant organs and their biochemical fractions using NMR

Subsamples of the biochemical fractions (HWE, TSE, CF and AUR) obtained from each plant organ (leaves, twigs, bark, wood and roots) were analyzed in an isotope ratio mass spectrometer – IRMS (ANCA-GSL, 20-20, Sercon, Crewe-UK) to determine their total contents of C, N and ^{13}C enrichment. Isotopic data were referred to a V-PDB international standard and are also expressed in ^{13}C-atom% notation. Total

carbon, nitrogen, C:N ratio, and isotopic data of each biochemical fraction are given in Table 2.

The molecular composition of each plant organ and biochemical fractions was determined using solid-state ^{13}C cross-polarization magic angle spinning (CPMAS) NMR spectroscopy (Bruker DSX 200 spectrometer, Bruker BioSpin GmbH). Accordingly, the samples were filled into zirconium dioxide rotors and the measurements conducted at a rotation speed of 6.8 kHz, with a 'magic angle' around 54.74°, acquisition time of 0.01024 s and a delay time of 1.0 s. All spectra were integrated along seven integration areas: 0–45 ppm (Alkyl C), 45–60 ppm (N-Alkyl/Methoxyl C), 60–95 ppm (O-Alkyl C), 95–110 ppm (Di-O-Alkyl C), 110–145 ppm (Aromatic C), 145–165 ppm (Phenolic C) and 165–215 ppm (Amide/Carboxylic C). These integration areas for each plant organ and their respective biochemical fractions are given in Supplementary Fig. 1 for reference. In combination with total C and N content of each sample analyzed (Table 2), our NMR data was used to estimate the relative abundance of the main organic groups namely: carbohydrate, protein, lignin, lipid, carbonyl using the molecular mixing model (NELSON; BALDOCK, 2005). We further refer to this method in this text as NMR-MMM.

Table 2. Mean and standard error for total carbon, nitrogen, C:N ratio, and isotopic data expressed in $\delta^{13}C\text{-}_{PDB}$ and ^{13}C-atom% of each biochemical fraction (BF) extracted from leaves, twigs, bark, wood, and root tissues of eucalypt seedlings

Plant organ	BF	C, g kg^{-1}	N, g kg^{-1}	C:N	$\delta^{13}C\text{-}_{PDB}$	^{13}C-atom%
Leaves	HWE	421.2 ± 10.3	4.2 ± 0.2	100	324.4 ± 22.6	1.5 ± 0.0
	TSE	694.4 ± 2.9	4.6 ± 0.6	152	504.4 ± 43.0	1.7 ± 0.0
	CF	427.7 ± 11.1	2.5 ± 1.0	173	501.9 ± 28.6	1.7 ± 0.0
	AUR	588.2 ± 4.0	41.6 ± 2.4	14	441.5 ± 36.3	1.6 ± 0.0
Twigs	HWE	397.8 ± 6.4	4.7 ± 0.3	85	319.0 ± 12.0	1.5 ± 0.0
	TSE	731.9 ± 3.6	3.1 ± 0.2	239	379.7 ± 6.2	1.5 ± 0.0
	CF	420.3 ± 3.3	0.3 ± 0.1	1401	361.6 ± 21.3	1.5 ± 0.0
	AUR	570.8 ± 5.5	22.4 ± 1.1	26	382.4 ± 7.8	1.5 ± 0.0
Bark	HWE	407.9 ± 3.7	2.6 ± 0.1	157	276.1 ± 1.7	1.4 ± 0.0
	TSE	737.5 ± 10.7	3.4 ± 0.3	217	334.1 ± 12.9	1.5 ± 0.0
	CF	408.6 ± 1.8	0.5 ± 0.1	817	368.0 ± 18.7	1.5 ± 0.0
	AUR	560.9 ± 6.8	18.3 ± 1.5	31	312.9 ± 10.9	1.5 ± 0.0
Wood	HWE	343.8 ± 3.7	6.6 ± 0.4	52	229.2 ± 7.3	1.4 ± 0.0
	TSE	661.6 ± 8.6	4.9 ± 0.1	134	290.8 ± 6.1	1.4 ± 0.0
	CF	412.4 ± 2.9	0.5 ± 0.0	773	332.7 ± 45.3	1.5 ± 0.1
	AUR	574.0 ± 2.9	6.0 ± 0.3	95	375.8 ± 6.0	1.5 ± 0.0
Roots	HWE	400.9 ± 2.6	5.6 ± 0.6	72	302.2 ± 26.9	1.4 ± 0.0
	TSE	738.9 ± 2.4	2.0 ± 0.1	369	373.9 ± 25.8	1.5 ± 0.0
	CF	406.3 ± 3.3	1.2 ± 0.0	339	326.9 ± 33.4	1.5 ± 0.0
	AUR	552.1 ± 3.0	16.0 ± 2.0	34	342.1 ± 32.2	1.5 ± 0.0

HWE: hot water extractables; TSE: total solvent extractables; CF: cellulosic fraction; AUR: acid unhydrolyzable residue.

2.3.4. Characterization of biochemical fractions using thermochemolysis

We treated subsamples of each biochemical fraction with tetramethylammonium (TMAH) as described elsewhere in previous studies (ALMEIDA et al., 2018; HATCHER et al., 1995) and the products of the thermochemolysis were analyzed by off-line gas chromatography-mass spectrometry (GC-MS) in a Shimadzu QP 2010-SE GC-MS equipped with a Rtx-5MS column (30 m length; 0.25 mm ID; 0.25 µm film thickness). We used ultrapure He as the carrier gas (3 mL min^{-1}) and set the temperatures of the ion source and the interface to 200 °C and 290 °C, respectively. For the oven, its temperature was ramped in the range between 60 °C and 300 °C (15 °C min^{-1}), and the initial and final analysis time were set to start at 3.50 min and finish at 48.5 min. As external standards, we used 3,5-dimethoxy-4-hydroxyacetophenone; syringaldehyde; syringic acid; ferulic acid; vanillic acid; p-coumaric acid; 3-

hydroxybenzaldehyde; 4-hydroxyacetophenone; 3,4-dihydroxybenzoic acid. We also used a NIST 2011 mass spectral library to identify the compounds eluted in our study with a minimum similarity index (SI) arbitrarily set at 85%. Subsequently, we used the molecular formula of each compound identified to obtain the number of atoms of C, H, O, and N in their structure. We used this data to calculate the weighed element content (WEC) according to the following formula:

$$WEC = nA \times PA/100$$

where nA is the number of atoms (C, H, O or N) and PA is the peak area of each compound in the mixture, which total sum was 100%. Thus, WEC is a metric that corrects the number of atoms in a given compound by taking into account its relative contribution to the total ion intensity measured.

2.3.5. Incubation experiment

We used the biochemical fractions (HWE, TSE, AUR and CF) to incubate soil samples under controlled conditions 25 ± 1 °C. Neither the wood tissue nor its biochemical fractions were included in the incubation study. In total, we had factorial 4 × 4 (four biochemical fractions extracted from leaves, twigs, bark and roots) and a control treatment with only soil material. We had three replicates in total.

For the incubation experiment itself, each plant organs were “reconstructed” in a way that each biochemical fraction occurred at 25% (corrected for C content). This was done because in the original plant organs, the proportion of each biochemical fraction was different, and we opted to keep all of them at fixed proportion to minimize this effect in the experimental results. Moreover, for a given “reconstructed” organ, only one of the four biochemical fractions was isotopically labeled. For instance, in order to “reconstruct” the leaf material, the ^{13}C-enriched leaf-HWE was mixed with the other three fractions (TSE, CF, and AUR) obtained from leaf tissues of unlabeled plants. The same strategy was used for the other biochemical fractions of leaves and also for the other “reconstructed” organs. This approach allowed us to determine the extent to which the respiration of a specific biochemical fraction would be impacted by its inherent molecular properties in the presence of other biochemical fractions. All

"reconstructed" plant organs were added to soil samples at a rate of 10.0 g C kg^{-1} of soil.

We incubated the artificial plant organs obtained in soil samples collected from the A horizon (0−20 cm depth) of a sandy-loam Haplic Ferralsol (IUSS WORKING GROUP WRB, 2015). This soil had pH (measured in H_2O) about 5.65 and 4.6 (measured in KCl); P content was 3.60 mg dm^{-3} soil; exchangeable K, Ca and Mg contents were about 0.22, 1.8 and 1.2 ($cmol_c$ dm^{-3}), respectively; Total sand, clay and silt contents were 520.0, 310.0 and 170.0 g kg^{-1} soil, respectively. Kaolinite was the predominant clay mineral (220.0 g kg^{-1} soil); and the original soil organic carbon content was 22.20 g kg^{-1} soil and $\delta^{13}C$ about −16.00 ‰. Water holding capacity (WHC) was 0.2 g g^{-1} soil and during the incubation of the samples their moisture content was kept at 80.0% of WHC. For the incubation, we placed 20 g of the soil material (particle-size <2.0 mm) into 0.57 L air-tight glass jars with lids containing a rubber septum, from which we sampled the air in the headspace to monitor C-CO_2 evolution. Over the course of the incubation experiment, we assessed soil respiration at 0.25, 0.50, 1, 2, 3, 4, 7, 10, 13, 21, 28, 38, 45, 70, 80, 92, 112, 148, 178 and 200 days after the incubation began. This data was subsequently grouped into the following time intervals: 0–2; 2–10; 10–38; 38–92; 92–200 days, hence each interval included four individual samplings. For each sampling, we collected an aliquot containing 100-mL of air from the headspace of each jar and analyzed the gas sample to determine $^{13}C/^{12}C$-CO_2 concentrations in a cavity ring-down spectrometer (CRDS, G2131-i, Picarro, Sunnyvale, CA). After each sampling, we vented the jars, checked soil moisture content and kept the experimental units closed until the subsequent assessment. We used the data from our $^{13}C/^{12}C$-CO_2 measurements to determine the proportion C-CO_2 derived using the following formula:

$$f = (\delta_{tbf} - \delta_{co})/(\delta_{bf} - \delta_{co})$$

where f is the proportion of C-CO_2 from a given biochemical fraction; δ_{tbf} is the $\delta^{13}C$ of the CO_2 respired from the treatments receiving isotopically labeled biochemical fractions; δ_{bf} is the $\delta^{13}C$ of each biochemical fraction; and δ_{co} is the $\delta^{13}C$ of the CO_2 respired from the control treatment.

2.3.6. Statistics

The results for C, N and ^{13}C as well as the relative abundance of main organic groups in plant organs and biochemical fractions were submitted to analysis of variance (ANOVA) and the means values were compared by Tukey's test ($p<0.05$). We used correlation analysis to determine the relationship between the respiration of the biochemical fractions for each sampling interval and quantitative parameters obtained from our calculations based on NMR-MMM and thermochemolysis-GC-MS. We set the significance level for the Pearson's correlation coefficients obtained at $p<0.05$. All statistical analyses were performed in Statistica STATSOFT 2013 (Palo Alto, CA, USA) and we used Sigma Plot 11.0 (San Jose, CA, USA) to draw the figures.

2.4. Results

2.4.1. Molecular chemistry of bulk plant tissues based on NMR-MMM

We used NMR-MMM to assess the molecular chemistry of bulk plant organs in order to set a base reference for their biochemical fractions (Fig. 1). Accordingly, our NMR-MMM results indicate that bulk leaves had less than 40% of carbohydrates, whereas these compounds were close to 60% in the other organs evaluated (Fig. 1A). Otherwise, leaves had comparatively more proteins (about 10%) and lipids (about 20%), both of which accounted for less than 10% of the bulk chemistry of the other organs evaluated. Generally, carbohydrates and lignin were the most abundant materials in all plant organs evaluated (Fig. 1A). As expected, carbohydrates were particularly important for bulk wood tissues and accounted for more than 70% of their bulk chemistry, whereas lipids and lignin contents were very low. Moreover, twigs and bark presented similar biochemical composition, except for the comparatively higher amounts of lignin and lipids found in bulk bark tissue (Fig. 1A).

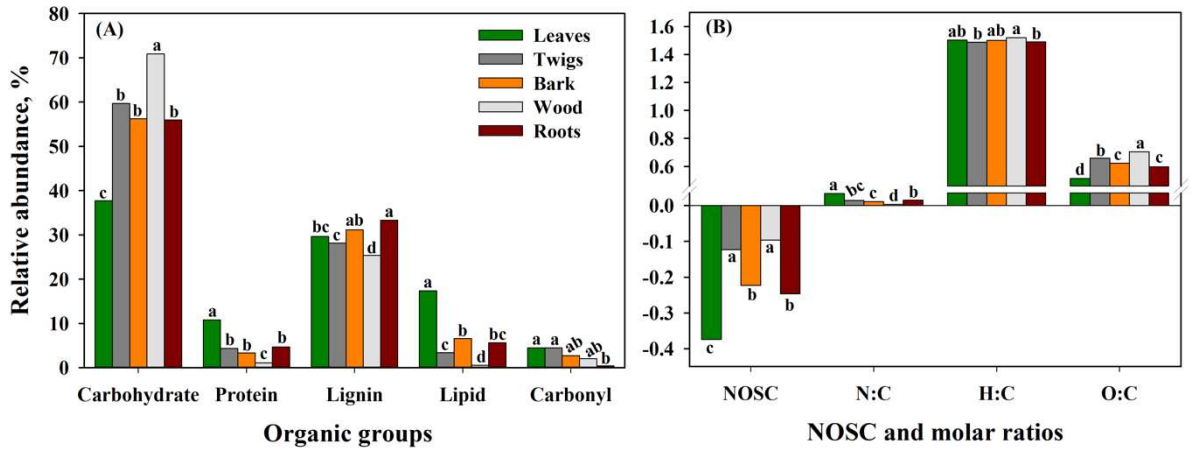

Fig. 1. Biochemical characterization of ^{13}C enriched eucalypt plant organs based on nuclear magnetic resonance (NMR) spectroscopy and the Molecular Mixing Model (NELSON; BALDOCK, 2005); A) Relative abundance of the main organic groups within leaves, twigs, bark, wood and roots of eucalypt plants; B) Nominal Oxidation State of Carbon (NOSC) and molar ratios (N/C; H/C and O/C) of leaves, twigs, bark, wood and roots of eucalypt plants. For a given organic group, NOSC or molar ratio, means followed by the same lowercase letter do not differ at $p<0.05$ (Tukey's test).

Our NMR-MM results also indicated that bulk leaves would have had the lowest NOSC (–0.37), with bark and roots showing intermediary values (–0.22 and –0.25, respectively) (Fig. 1B). Twigs and wood had the highest NOSC values, about –0.12 and –0.10, respectively (Fig. 1B). Additionally, leaves also had the highest N:C ratio, which was intermediary for twigs, bark and roots, and lowest for wood. Moreover, the H:C ratio was relatively uniform among plant organs, whereas their O:C ratio tended to vary more (Fig. 1B). As such, wood presented the highest O:C ratio (0.71) followed by twigs (0.66), bark and roots (0.62 and 0.60, respectively), and leaves (0.51) (Fig. 1B).

2.4.2. Composition of the biochemical fractions as inferred from NMR-MMM results

Our NMR-MMM data indicates that the biochemical composition of each biochemical fraction varied according to the plant organ source (Fig. 2). Generally, materials extracted within the HWE fraction were dominated by lignin (48.1–61.3%) and carbohydrates (31.0–42.8%), whereas protein (2.0–5.7%), carbonylic C (2.1–5.6%), and lipids (1.0–3.0%) were less abundant (Fig. 2A). For this fraction, the most evident difference observed among the organs was that the HWE of roots that had

more carbohydrates and less lignin (Fig. 2A). Within the TSE fraction, lipids (62.7–90.7%%) and lignin (7.9–27.9%) were predominant, with minor proportions of proteins (0.9–2.2%) (Fig. 2B). In this case, the TSE of roots had more lignin and less lipids than the other organs (Fig. 2). For the structural fractions, CF was predominantly composed by carbohydrates (86.3–89.6%) and lignin (7.4–9.5%), with a small proportion of carbonylic C varying between 1.4–2.4% (Fig. 2C). Generally, the CF was the most homogeneous among the plant organs and exhibited similar proportions of carbohydrates and lignin (Fig. 2C). Otherwise, the AUR fraction also had some carbohydrates (2.4–10.6%). Overall, the AUR fraction tended be more heterogeneous in terms of its constituents as compared to the other biochemical fractions (Fig. 2D). As expected, the AUR was dominated by lignin in twigs (65.9%), bark (64.0%), wood (71%.) and roots (86.6%), whereas in leaves this total was about 36.5% (Fig. 2D). In addition, the AUR of leaves also had substantial amounts of proteins (23.6%) and lipids (36.5). For the other organs, their AUR had proteins and lipids varying between 3.9–13.3% and 10.1–17.6%, respectively. Only roots had no detectable amount of lipids in their AUR (Fig. 2B).

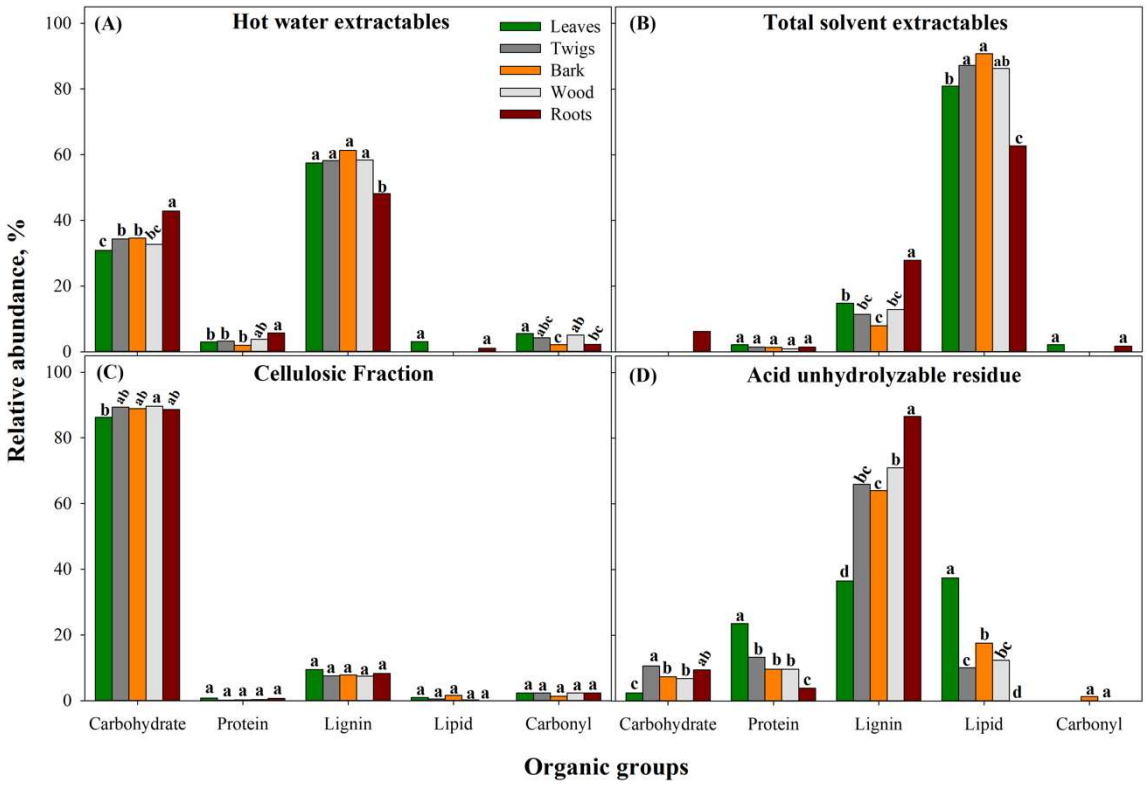

Fig. 2. Relative abundance of the main organic groups (carbohydrate, protein, lignin lipid and carbonyl) within the biochemical fractions extracted from leaves, twigs, bark, wood and roots of eucalypt plants as determined by NMR spectroscopy and the

Molecular Mixing Model (NELSON; BALDOCK, 2005); A) hot water extractables; B) total solvent extractables; C) cellulosic fraction and D) acid unhydrolyzable residue. For a given organic group within the same biochemical fraction, means followed by the same lowercase letter do not differ at $p<0.05$ (Tukey's test).

In terms of NOSC, the CF showed the highest averaged values (–0.02), followed by HWE (–0.20), AUR (–0. 49), and TSE showed the lowest averaged values (–1.27) as shown in Fig. 3A. Additionally, we also observed significant differences in NOSC values of TSE and AUR depending on the plant organ source. As such, TSE and AUR presented higher NOSC values in roots as compared to other plant organs, whereas the TSE of twigs and bark, and the AUR of leaves had the lowest NOSC values (Fig. 3A). Moreover, constituents of the AUR had the highest N:C ratio, followed by HWE, TSE and CF (Fig. 3B). For HWE and AUR specifically, the N:C ratio was significantly affected by plant organs, while TSE and CF presented similar N:C ratios for all plant organs. Accordingly, the HWE of roots showed higher N:C ratio than the other plant organs, whereas the highest N:C ratio in the AUR was observed for leaves and the lowest values occurred in roots (Fig. 3B). Further, H:C ratio was highest in TSE (1.83), intermediate in CF (1.61) and similar for HWE (1.36) and AUR (1.37) (Fig. 3B). Finally, the CF showed the highest O:C ratio (>0.75) and the lowest values occurred for the constituents of the TSE (about 0.25). For the compounds within the HWE, their O:C ratios varied between 0.50–0.55 for all plant organs. Otherwise, the O:C ratios of the AUR varied between 0.28 for leaves up to 0.45 for roots (Fig. 3B).

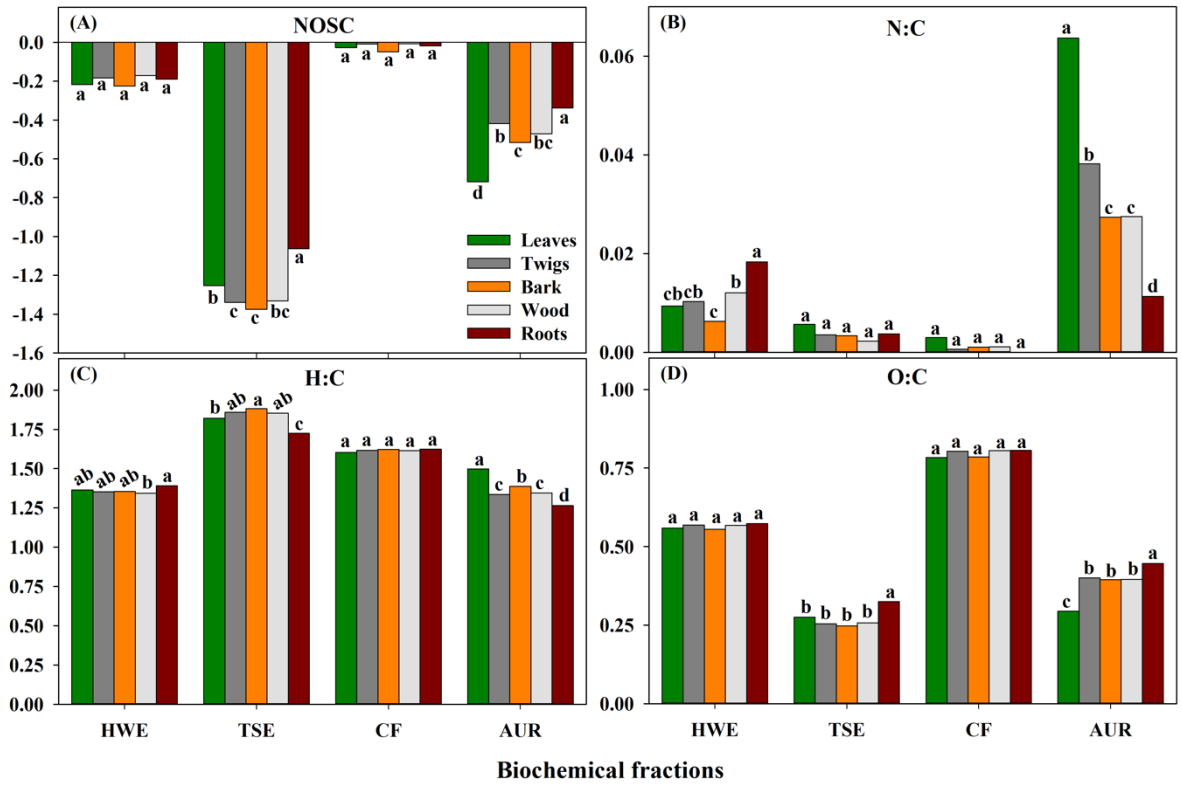

Fig. 3. Chemical characteristics of the biochemical fractions extracted from leaves, twigs, bark, wood and roots of eucalypt plants as determined by NMR spectroscopy and the Molecular Mixing Model (NELSON; BALDOCK, 2005); A) Nominal oxidation state of carbon (NOSC); B) nitrogen to carbon ratio (N:C), C) hydrogen to carbon ratio (H:C) and D) oxygen to carbon ratio (O:C). HWE — hot water extractables, TSE — total solvent extractables, CF — cellulosic fraction and AUR — acid unhydrolyzable residue. For a given biochemical fraction within the same chemical characteristic, means followed by the same lowercase letter do not differ at $p<0.05$ (Tukey's test).

2.4.3. Molecular weight of the constituents of each biochemical fraction

Upon the separation and identification of the major constituents of each biochemical fraction, we used their reduced chemical formula to obtain the number of C, H, and O atoms in each molecule. Curiously, N-bearing compounds were mostly absent in our GC-MS data, even for the AUR fraction that had high N content as indicated by the NMR results (Fig. 2D). Moreover, grouping the organic compounds identified in our GC-MS in classes including short (≤10 C atoms), mid (10 < C atoms <30), and long C chains (≥30 C atoms), facilitated comparing all biochemical fractions among themselves (Table 3). All WEC values for C, H, and O in short, mid and long chains are given in Table 4.

Table 3. Proportion (%) of short (≤ 10 C atoms), mid (10 < C atoms < 30) and long C chains (≥ 30 C atoms) among the constituents of each biochemical fraction, namely hot water extractables (HWE), total solvent extractables (TSE), cellulosic fraction (CF), and acid unhydrolyzable residue (AUR) obtained from leaves, twigs, bark, and roots of eucalypt seedlings

Carbon chain		**short**		**mid**		**long**	
Plant organ	Biochemical fraction	n†	Proportion, %	n†	Proportion, %	n†	Proportion, %
Leaves	HWE	24	57.4	20	42.6	0	0.0
	TSE	0	0.0	27	55.1	8	44.9
	CF	21	65.6	15	32.2	1	2.2
	AUR	6	3.6	28	88.5	2	8.0
Twigs	HWE	16	56.4	11	43.6	0	0.0
	TSE	1	0.1	23	68.0	6	31.8
	CF	17	60.2	16	39.8	0	0.0
	AUR	5	11.4	28	82.2	1	6.4
Bark	HWE	15	77.2	8	22.8	0	0.0
	TSE	1	0.1	31	80.5	7	19.4
	CF	22	71.3	20	28.6	1	0.1
	AUR	6	4.5	24	91.0	4	4.5
Roots	HWE	15	55.2	14	44.8	0	0.0
	TSE	3	0.6	42	95.3	2	4.1
	CF	23	77.2	15	22.8	0	0.0
	AUR	4	2.8	23	93.6	2	3.5

†n: Number of compounds identified.

Table 4. Weighed element content (WEC) for C, H, and O of the constituents identified grouped in short (≤ 10 C atoms), mid (10 < C atoms < 30) and long C chains (≥ 30 C atoms) for each biochemical fraction (BF) namely, hot water extractables (HWE), total solvent extractables (TSE), cellulosic fraction (CF), and acid unhydrolyzable residue (AUR) obtained from leaves, twigs, bark, and roots of eucalypt seedlings

Carbon chains		**short**				**mid**				**long**			
Plant organ	BF	n†	C	H	O	n†	C	H	O	n†	C	H	O
Leaves	HWE	24	8	14	4	20	16	28	5	0	0	0	0
	TSE	0	0	0	0	27	25	51	2	8	31	57	3
	CF	21	9	16	5	15	15	28	6	1	31	62	2
	AUR	6	9	13	4	28	22	44	2	2	32	64	2
Twigs	HWE	16	8	14	4	11	15	25	6	0	0	0	0
	TSE	1	10	12	4	23	24	48	1	6	31	57	2
	CF	17	9	17	5	16	15	29	7	0	0	0	0
	AUR	5	10	12	4	28	20	38	3	1	31	62	2
Bark	HWE	15	8	15	4	8	16	24	5	0	0	0	0
	TSE	1	10	12	2	31	25	51	2	7	31	58	2
	CF	22	9	16	5	20	18	34	8	1	38	68	8
	AUR	6	9	12	4	24	23	46	2	4	32	62	4
Roots	HWE	15	7	12	2	14	16	29	2	0	0	0	0
	TSE	3	10	11	4	42	21	41	2	2	31	56	3
	CF	23	9	16	4	15	18	35	6	0	0	0	0
	AUR	4	10	12	4	23	22	44	2	2	32	62	4

†n: Number of compounds identified.

Our GC-MS data shows that the WEC for C varied in the range between 9.9–11.7 for HWE and 10.7–11.5 for CF, whereas these values were comparatively higher within the AUR (19.4–22.8) and TSE (21.3–27.9) fractions (Fig. 4). Therefore, short C chains within the HWE and CF accounted for approximately 55.2 and 77.2% of their respective total peak area measured (Table 3). Moreover, the total peak area accounted for by mid C chains were comparatively lower than short C chains for both HWE and CF (Table 4). Further, except for the CF of leaves, these fractions also had no compounds with log C chain. Otherwise, mid and long C chains were much more abundant in TSE and AUR, consistent with their WEC for C, H, and O (Fig. 4). Importantly, mid C chains within the TSE fraction varied substantially depending on the plant organ (Table 3). As such, leaves had the smallest proportion of mid C chains (55.0%), whereas in twigs, bark, and roots these compounds reached about 68.0, 81.0, and up to 95.0% of the total signal intensity, respectively (Table 3). In contrast, long C chains were more abundant in the TSE of leaves (44.9%), twigs (31.8%), bark (19.4%),

and comparatively less frequent in roots (4.1%) (Table 3). Mid C chains were predominant within the AUR and accounted for between 82.0 and 94.0% of the total peak area identified in our GM-MS data (Table 3). Although long C chains also were observed within the AUR, these compounds accounted for no more than 8.0% of the total peak area (Table 3).

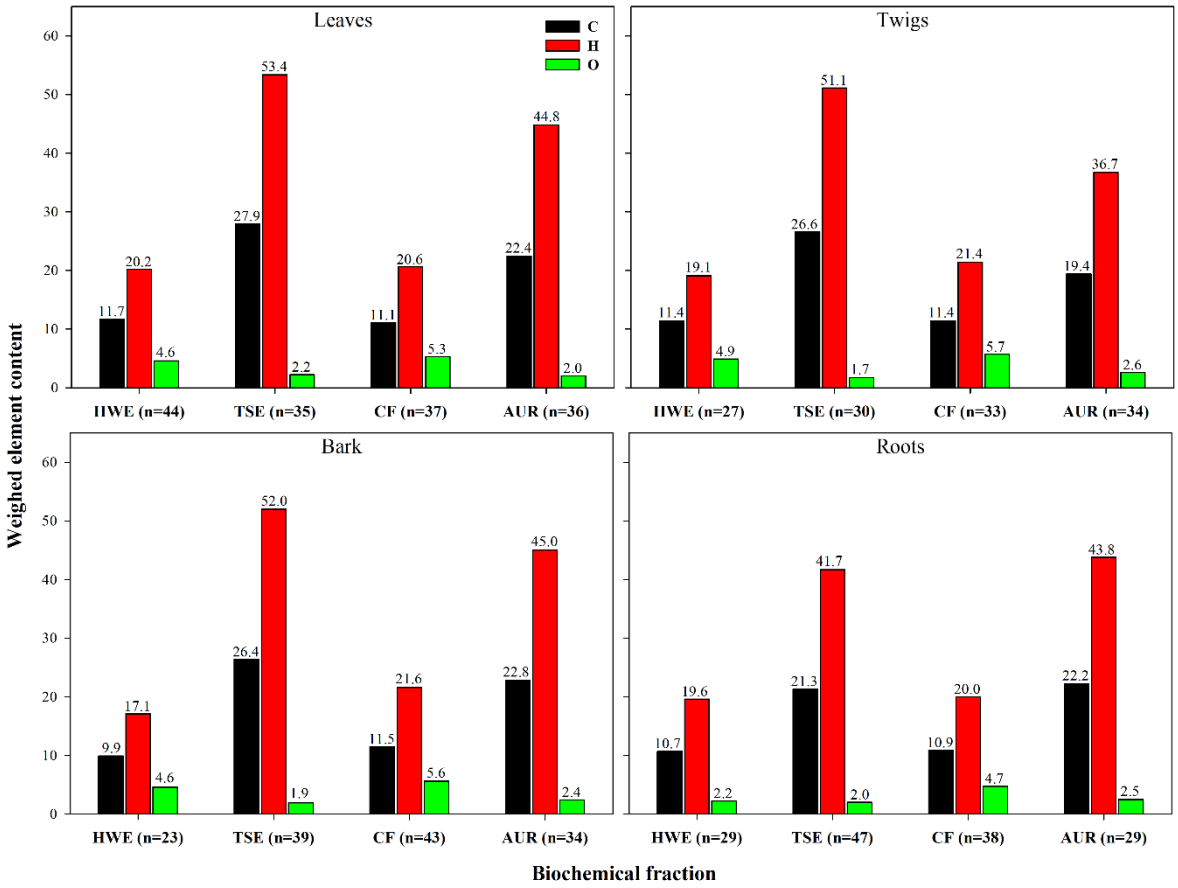

Fig. 4. Weighed element content (C, H, and O) for hot water extractables (HWE), total solvent extractables (TSE), cellulosic fraction (CF), and acid unhydrolyzable residue (AUR) obtained from leaves, twigs, bark, and roots of eucalypt seedlings. Numbers above the bars indicate the weighed element mass corrected by the relative intensity of each compound identified in the mixture.

In order to complement the WEC data given in Table 4, we also calculated the O:C ratio for the compounds identified in our GC-MS analysis (Fig. 5). Generally, short C chains also tended to exhibit narrow O:C ratios than mid and especially long C chains. Except for the TSE of leaves, all biochemical fractions had at least one compound with O:C ratio in the range between 0.2 and 0.6 (Fig. 5). For mid C chains, HWE and CF showed O:C ratios between 0.3 and 0.5, except for roots, which O:C ratio was about 0.1. This value was similar to those observed for mid C chains within

the TSE and AUR fractions (Fig. 5). All long C chains showed O:C ratios below 0.2 consistent with their WEC for H (Table 4). Overall, the O:C ratio obtained from our GC-MS experiment and the C chain groups complemented and detail the O:C ratio as informed by the NMR data (Fig. 3).

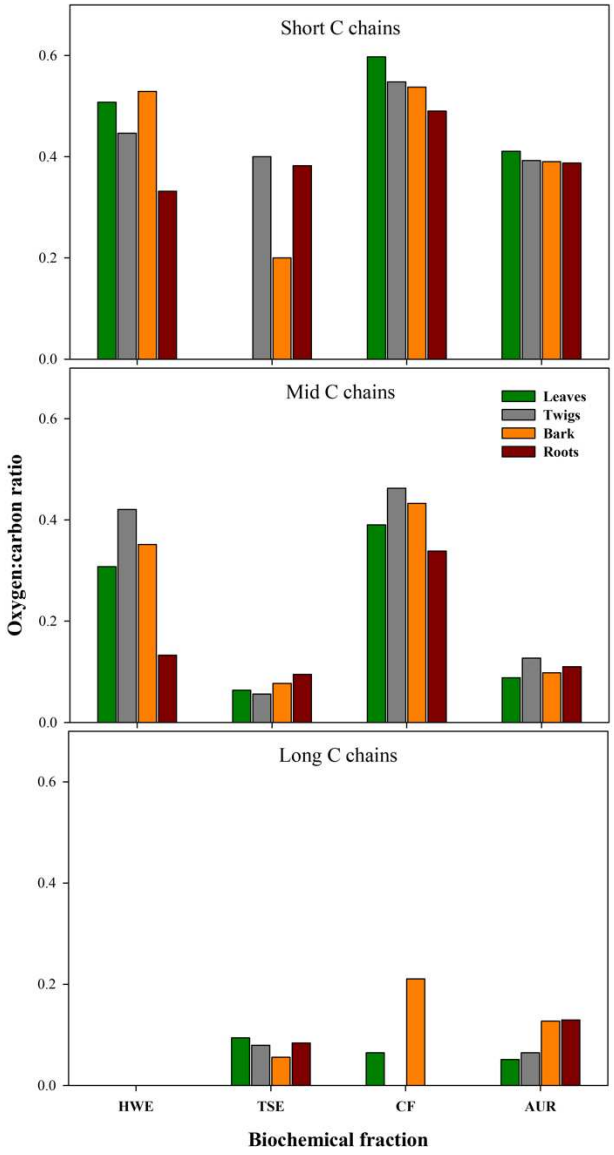

Fig. 5. Molar O:C ratios of short (≤ 10 C atoms), mid (10 < C atoms < 30) and long C chains (≥ 30 C atoms) of the constituents of hot water extractables (HWE), total solvent extractables (TSE), cellulosic fraction (CF), and acid unhydrolyzable residue (AUR) obtained from leaves, twigs, bark, and roots of eucalypt seedlings.

2.4.4. Microbial respiration on each biochemical fraction

Given the specific experimental setup of our study, we report the C-CO_2 derived from each 'reconstructed' plant organ and their respective biochemical fractions as a percentage of total soil respiration (Fig. 6). As such, over the course of the first two days of the experiment, soil microbes respired mostly the HWE fraction for all plant organs. Generally, the respective release of C-CO_2 from the HWE of leaves and twigs contributed to 37.9% and 31.0% of total soil respiration. Otherwise, the contribution for C-CO_2 from HWE in bark and roots were about 16.0% and 21.2%, respectively (Fig. 6). For the subsequent time interval (2-92 days), the contribution of HWE to total soil respiration was reduced and varied between 7.3% and 23.3% for all plant organs (Fig. 6). As the respiration of HWE decreased, the contribution of C-CO_2 derived from CF increased and became predominant, varying between 12.9 up to 44.5% of total soil respiration in the interval between 2-92 days of the experiment (Fig. 6). After 92 days of incubation, the HWE fraction remained an important contributor to total soil respiration for all plant organs (about 16% for leaves and 14.5% for twigs), but comparatively smaller for bark (8.3%) and roots (9.6%). Over the last 108 days of incubation, TSE was the main C source from bark (23.0%) and roots (27.0%) but represented only 3.1 and 5.8% of the soil C-CO_2 for leaves and twigs, respectively (Fig. 6). Overall, the AUR fraction showed the least contribution to total soil C-CO_2 emissions over the incubation experiment was less than 3.75%, averaging about 0.55% (Fig. 6).

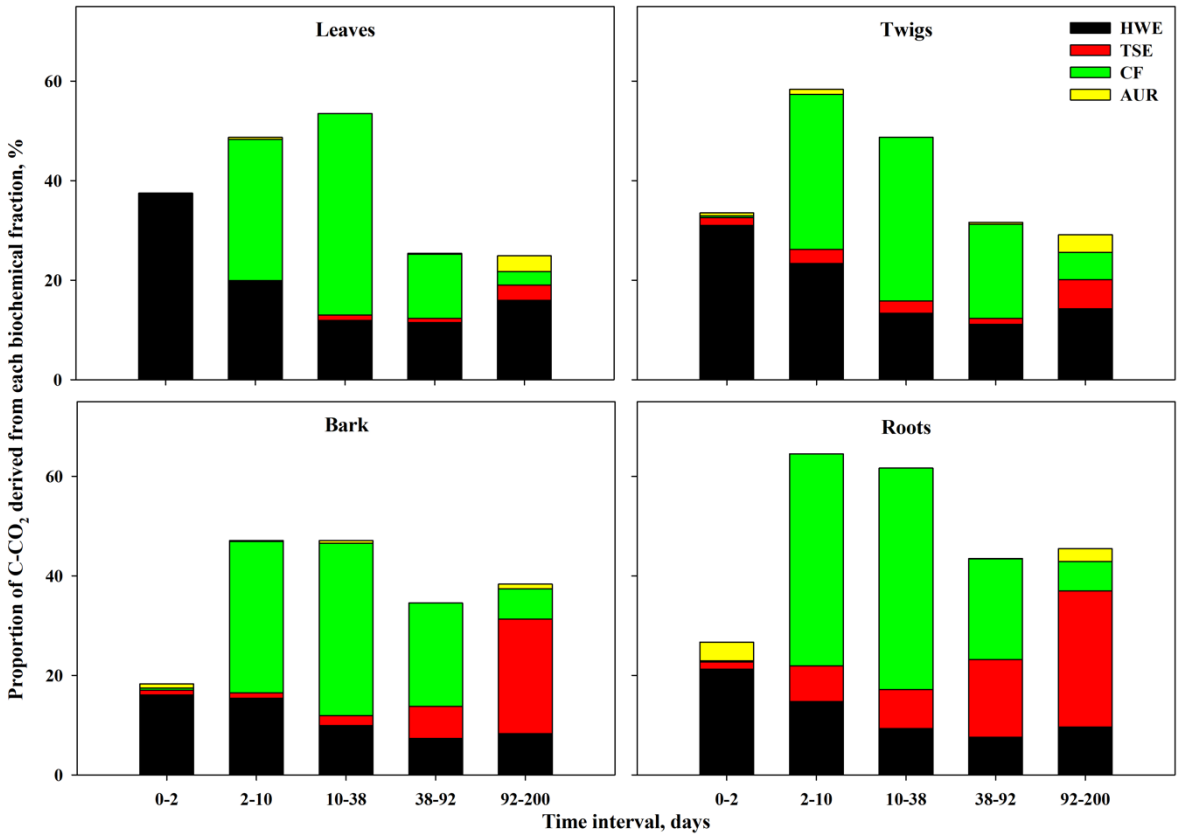

Fig. 6. Proportion of C-CO_2 derived from each biochemical fraction as a percentage of total soil respiration over the course of 200 days of the incubation experiment. Leaves, twigs, bark, and roots were 'reconstructed' using 25% of each biochemical fraction namely, hot water extractables (HWE), total solvent extractables (TSE), cellulosic fraction (CF), and acid unhydrolyzable residue (AUR).

2.4.5. Properties of the biochemical fractions and their respiration rates

Over the first four samplings, (0.25-2 days), the release of C-CO_2 from the biochemical fractions showed positive correlation ($r = 0.77$, $p<0.001$) with carbonylic C as inferred from the NMR data (Table 5). Moreover, the respiration rates observed were negatively correlated to H:C ratios (NMR data) and the proportion of long C chains (thermochemolysis data) as shown in Table 5. For the time interval between 2-10 days, the positive correlation between carbonylic C and the respiration of the biochemical fractions remained significant ($r = 0.58$, $p<0.018$), but not afterwards (Table 5).

Bulk properties (C and N content) showed significant ($p<0.05$) and negative correlations with the release of C-CO_2 from the biochemical fractions for the interval of

the incubation between 2 and 92 days. Simultaneously, the C:N ratio was positively correlated with the respiration of the biochemical fractions (Table 5). However, the release of C-CO_2 from the biochemical fractions showed comparatively stronger and positive correlations with their O:C ratio, carbohydrates content, short C chains, and the O:C of ratio of both short and mid C chains (Table 5). Among these variables, carbohydrates showed the highest correlations coefficients (0.94, 0.96, and 0.81) for the time intervals between 2-10, 10-38, and 38-92 days, respectively (Table 5). Other variables showed less consistent correlations with the release of C-CO_2 from the isotopically labeled substrates. For instance, NOSC showed strong and positive correlation with C-CO_2 emissions only for the time intervals between 2-10 (r = 0.71, $p<0.002$) and 10-38 days (r = 0.63, $p<0.008$) of the incubation (Table 5). Otherwise, lignin content was negatively correlated (r = –0.52 and –0.53, $p<0.05$) with the respiration of the biochemical fractions between 10-38 and 38-92 days (Table 5). Similar correlation coefficients were observed for the percentage of long C chains and C-CO_2 emissions, but significant values only occurred for the samplings made between 2-10 and 38-92 days (Table 5).

Overall, none of the variables included in our analysis showed significant correlations ($p<0.05$) with C-CO_2 emissions from the biochemical fractions for the time interval between 112-200 days of the incubation experiment (Table 5).

Table 5. Pearson's correlation coefficients (*r*) between selected properties of the biochemical fractions (BF) and their percentual contribution to total C–CO_2 emissions for each time interval: 0–2, 2–10, 10–38, 38–92, and 92–200 days of the incubation. Correlation coefficients significant at $p<0.05$ are indicated in bold typing.

Data source	Variable	0–2 days	2–10 days	10–38 days	38–92 days	92–200 days
Bulk properties	Carbon, g kg^{-1}	–0.48; p=0.059	**–0.76; p=0.001**	**–0.63; p=0.009**	**–0.51; p=0.045**	0.29; p=0.277
	Nitrogen, g kg^{-1}	–0.19; p=0.472	**–0.55; p=0.028**	**–0.51; p=0.043**	**–0.64; p=0.008**	–0.37; p=0.154
	C:N ratio	–0.27; p=0.310	**0.54; p=0.032**	**0.58; p=0.019**	**0.68; p=0.004**	0.02; p=0.948
NMR†	NOSC	0.32; p=0.230	**0.71; p=0.002**	**0.63; p=0.008**	0.46; p=0.075	–0.41; p=0.116
	N:C ratio	–0.07; p=0.787	–0.47; p=0.067	–0.47; p=0.064	**–0.57; p=0.020**	–0.33; p=0.212
	H:C ratio	**–0.50; p=0.047**	–0.06; p=0.839	0.10; p=0.718	0.20; p=0.459	0.37; p=0.161
	O:C ratio	0.15; p=0.582	**0.92; p=0.000**	**0.90; p=0.000**	**0.74; p=0.001**	–0.28; p=0.291
	Carbohydrates, %	0.00; p=0.993	**0.94; p=0.000**	**0.96; p=0.000**	**0.81; p=0.000**	–0.24; p=0.375
	Proteins, %	–0.10; p=0.699	–0.48; p=0.060	–0.48; p=0.062	**–0.58; p=0.020**	–0.33; p=0.218
	Lignin, %	0.47; p=0.066	–0.37; p=0.159	**–0.52; p=0.039**	**–0.53; p=0.035**	–0.20; p=0.448
	Lipids, %	–0.37; p=0.161	**–0.58; p=0.019**	–0.48; p=0.062	–0.31; p=0.248	0.43; p=0.094
	Carbonyl, %	**0.77; p=0.000**	**0.58; p=0.018**	0.39; p=0.134	0.41; p=0.117	0.06; p=0.820
TMAH/GC–MS‡	Short C chains, %	0.41; p=0.116	**0.90; p=0.000**	**0.79; p=0.000**	**0.72; p=0.002**	–0.08; p=0.756
	Short C chains O:C ratio	0.18; p=0.513	**0.64; p=0.007**	**0.61; p=0.011**	**0.54; p=0.032**	–0.13; p=0.637
	Mid C chains, %	–0.06; p=0.823	0.01; p=0.973	–0.05; p=0.849	0.04; p=0.897	0.07; p=0.801
	Mid C chains O:C ratio	0.30; p=0.256	**0.88; p=0.000**	**0.81; p=0.000**	**0.76; p=0.001**	–0.07; p=0.790
	Long C chains, %	–0.33; p=0.207	**–0.54; p=0.032**	–0.44; p=0.090	**–0.50; p=0.048**	–0.08; p=0.763
	Long C chains O:C ratio	**–0.53; p=0.034**	–0.30; p=0.257	–0.11; p=0.679	–0.14; p=0.592	–0.23; p=0.391

†Data obtained from nuclear magnetic resonance (NMR) spectroscopy; ‡Data obtained from thermochemolysis (TMAH) coupled to off–line gas–chromatography (GC) and mass spectrometry (MS).

2.5. Discussion

2.5.1. Molecular diversity: carbon bonds and molecular weight

In our analysis, our first goal was to obtain quantitative parameters to express the molecular diversity of the major constituents of each biochemical fraction obtained from eucalypt seedlings. These quantitative parameters were based on bulk element contents (Table 2), the predominant functional groups and related chemical properties (Fig. 2 and 3), and the size of the molecules in which these C bond types occurred (Fig. 4; Tables 3 and 4).

Generally, HWE, TSE, and CF showed chemical composition consistent with what could be expected based on the extraction procedure used, although these fractions were not homogeneous. Accordingly, our NMR-MMM data indicated a significant proportion of 'lignin' within the HWE fraction, which may be explained by the extraction of phenolic such as monolignols (FREI, 2013). This inference is supported by the relatively low molecular weight of the constituents found within the HWE fraction (Fig. 4). According to the NMR-MMM, signal intensity from lignin is highest in the spectral range between 110 and 145 ppm (NELSON; BALDOCK, 2005). Consequently, it is very likely that all substances containing aromatic rings could have been pooled together as 'lignin' (Fig. 2). In fact, our findings are consistent with previous results showing a range of phenolic compounds within the water-soluble fraction of eucalypt leaf tissues (CHAPUIS-LARDY; CONTOUR-ANSEL; BERNHARD-REVERSAT, 2002; SANTOS et al., 2011). Moreover, carbohydrates (Fig. 2), substances showing low-molecular weight (Fig. 4) and high O:C ratio (Fig. 5) within the HWE and CF were expected. Likewise, the TSE fraction was dominated by lipids, long C chains with low O:C ratio, and minor proportions of 'lignin' according to the NMR-MMM. In this case, 'lignin' also may be accounted for the presence of phenols, but not in short C chains as observed for the HWE fraction (Table 3). For the TSE of leaves, twigs and bark, our WEC data indicated averaged C chains containing about 27 C atoms, consistent with previous studies on wax present in eucalypt leaf tissues (HOFFMANN et al., 2013; KNIGHT; WALLWORK; SEDGLEY, 2004; OSAWA; NAMIKI, 1985). Interestingly, the TSE fraction of roots had less lipids, more lignin and shorter C chains (about 21 C atoms) than aboveground tissues (Fig. 4). Overall,

hexadecanoic acid (C_{17}), methyl stearate (C_{19}), and 11-octadecenoic acid (C_{18}) accounted for by approximately 37% of total peak area of the compounds with C chains between 11 and 29 C atoms of the TSE fraction of roots. In addition, our estimates based on NMR-MMM indicated that some 'lignin' was released upon the treatment of the roots with acetone. Although aromatic C is an important constituent of suberin (KÖGEL-KNABNER, 2002), it is unclear whether the extraction with acetone could release structural components from root tissues. Previous reports indicate that suberin can be formed by approximately 30% of aliphatic C (C_{16}, C_{18}, C_{22}) and about 40-45% phenolics (KOLATTUKUDY, 1981). Our results would be in line with these findings.

In contrast to HWE, TSE, and CF, the AUR fraction was composed by a complex mixture of substances rather than 'pure lignin' consistent with previous findings (HILLI et al., 2012; PRESTON; TROFYMOW, 2015; SLUITER et al., 2010). Particularly important is the presence of N-rich substances within the AUR since pure lignin should not contain N (BRADLEY, 2002). Instead, the N content within the AUR obtained from plants in temperate ecosystems has been reported to vary between 3.0 and 9.0 g kg^{-1} (PRESTON; TROFYMOW, 2015). In our study, the AUR had N contents about 41.6, 22.4, 18.3, 2.0, and 16 g kg^{-1} in leaves, twigs, bark, stem wood, roots, respectively (Table 2). Unfortunately, only a few N-rich materials were identified in our thermochemolysis data, which cannot be used to complement the NMR results. Previous results on litter fractions obtained using proximate analysis also indicated small number of compounds containing N among pyrolysis-GC products (HILLI et al., 2012). According to our data, the protein content as inferred form the NMR-MMM approach was directly proportional to the N content, except for wood (Fig. 2). This result is also consistent with previous findings showing strong correlation between N and AUR contents for 79 broadleaf plant litter collected at latitudes varying from 11 °N and 70 °N (BERG et al., 2013). Beyond N-rich materials, the AUR fraction also had minor concentrations of carbohydrates and lipids, which were particularly relevant for leaves (Fig. 2). As expected, wood, twigs and bark had more lignin within their AUR (60-70%) than leaves (<40%), but considerably less than roots (about 90%). Furthermore, our WEC data also suggests that between 82.2 and 93.6% of the constituents of the AUR had between 11 and 29 C atoms (Table 3 and 4). Hence, despite the presence of carbohydrates, protein and lipids within the AUR fraction,

constituents of lignin were probably predominant (Fig. 2). Similar reports have been made for pine and spruce litter elsewhere (ZECH et al., 1987).

Overall, the use of thermochemolysis coupled to off-line GC-MS to obtain a quantitative assessment on the molecular weight of major constituents of biochemical fractions of plant tissues can be an important tool to complement the data for functional groups obtained in NMR-MMM.

2.5.2. Molecular diversity and substrate respiration in soil

Our data suggests that molecular diversity exerted a weaker effect on the respiration of the extractables (HWE and TSE) than the structural biochemical fractions (CF and AUR). Based on our NMR experiment and the functional groups identified therein, the CF showed the least molecular diversity (Fig. 2C) and the highest respiration rates among the fractions evaluated (Fig. 6). This is probably because the CF was dominated by carbohydrates with NOSC close to zero (Fig. 2) and abundant compounds with low molecular weight and high O:C ratio (Fig. 5). Hence, the constituents of the CF had low molecular diversity and no major constraints on their absorption and assimilation by soil microbes (HEDGES; KEIL, 1999; KLEBER et al., 2015). Otherwise, AUR showed the highest molecular diversity (Fig. 2D) and lower respiration rates than the other biochemical fractions studied (Fig. 6). Therefore, our results observed for CF and AUR are in line with the hypothesis that with increasing molecular diversity there is an increase in 'metabolic cost' for the assimilation of a given substrate or a mixture of them (LEHMANN et al., 2020). Three major aspects might contribute to link the high molecular diversity of AUR and its slow respiration (Fig. 6). Firstly, the predominance of hydrophobic constituents such as lignin and long chain lipids within the AUR (Fig. 2 and 3) might limit enzymatic attack and microbial respiration (Almeida et al., 2018). In part, this is because microbial respiration increases to produce more extracellular enzymes, whereas microbial growth yield is reduced (MALIK et al., 2019; RAMIN; ALLISON, 2019). Secondly, the adsorption of N-rich compounds of the AUR onto mineral surfaces could render these materials less susceptible to enzymatic attack (JILLING et al., 2018; KLEBER; SOLLINS; SUTTON, 2007; KOPITTKE et al., 2017). Third, it is possible that N-rich materials within the AUR could have been used in microbial anabolism to a greater extent than catabolism (KALLENBACH; FREY; GRANDY, 2016). This aspect is in line with weak or negative

correlations between substrate respiration and N:C ratio or protein content (Table 5). Regardless of the specific processes involved, it seems clear that the presence of energy-rich substrates in the mixture (e.g., CF and HWE), they had no detectable effects on the respiration of AUR. Otherwise, nothing can be said about whether or not N-rich materials within the AUR could have been assimilated by microbes as they respired HWE or CF.

Although molecular diversity as informed by NMR-MMM and thermochemolysis-GC-MS (Fig. 2–4) provided relevant parameters to compare the respiration of CF and AUR, the same cannot be said about the processing of HWE and TSE. This is because lipids accounted for more than 80% of the total signal intensity of TSE (except in roots, which had 60% lipids), whereas the highest frequency of a single functional group was not greater than 60% for the HWE fraction (Fig. 2). Hence, the lower molecular diversity of TSE should have favored its respiration relative to the HWE, but it did not (Fig. 6). As pointed out in earlier studies, thermodynamic constraints determined by substrate chemistry have a major influence on microbial respiration (HUANG et al., 2020; KEILUWEIT et al., 2016; LAROWE; VAN CAPPELLEN, 2011). Because the HWE had more polar constituents, its solubility probably favored its respiration at the very early stages of the experiment, but not necessarily limiting its respiration afterwards (Fig. 6). Furthermore, the constituents of TSE were dominated by longer C chains with reduced polarity and lower NOSC than the constituents of HWE (Fig. 3–5; Table 3). This is also consistent with previous evidence showing constrained activity of hydrolytic enzymes on the depolymerization long C chains, hampering both their assimilation and respiration by microbes (KEILUWEIT et al., 2016). In addition, the TSE of bark and roots were respired at higher rates than the same fraction extracted from leaves and twigs, both of which had more constituents with long C chain showing more than 30 C atoms (Table 3). Therefore, despite the relevance of the diversity of functional groups on microbial respiration, it is also critical to consider thermodynamic constraints (e.g., NOSC, substrate polarity), especially those related to the distribution of molecular weight of the constituents of a given substrate.

2.6. Conclusions

Our results showed complimentary information about the molecular diversity of the biochemical fractions of eucalypt plant tissues obtained from NMR-MMM and thermochemolysis-GC-MS experiments. Generally, the WEC data helped to improve our estimates based on NMR-MMM, especially for the HWE fraction in which aromatic C was attributed to lignin. Our data also suggests that molecular diversity is not always sufficient to predict microbial respiration of specific biochemical fractions of plant material. Indeed, the CF showed very low molecular diversity and was preferentially respired throughout the experiment. In sharp contrast, AUR showed the highest molecular diversity and was much less respired by soil microbes. However, the TSE fraction was dominated by lipids and long C chains, hence showing limited molecular diversity but was respired at low rates, especially for leaves and twigs. Furthermore, the CF showed lower molecular diversity than HWE, which was the first fraction attacked by microbes as the incubation started. Therefore, substrate selection and thermodynamic constraints on microbial metabolism are more relevant for the respiration of biochemical fractions of eucalypt plant tissues than their inherent molecular diversity.

2.7. References

ALMEIDA, L. F. J. et al. Soil organic matter formation as affected by eucalypt litter biochemistry — Evidence from an incubation study. **Geoderma**, v. 312, n. March 2017, p. 121–129, fev. 2018.

ANGST, G. et al. Soil organic carbon stocks in topsoil and subsoil controlled by parent material, carbon input in the rhizosphere, and microbial-derived compounds. **Soil Biology and Biochemistry**, v. 122, n. July, p. 19–30, 2018.

ANGST, G. et al. Soil organic carbon stability in forests: Distinct effects of tree species identity and traits. **Global Change Biology**, v. 25, n. 4, p. 1529–1546, 2019.

BERG, B. et al. Relationships between nitrogen, acid-unhydrolyzable residue, and climate among tree foliar litters. **Canadian Journal of Forest Research**, v. 43, n. 1, p. 103–107, 2013.

BIRD, J. A.; TORN, M. S. Fine Roots vs. Needles: A Comparison of 13C and 15N Dynamics in a Ponderosa Pine Forest Soil. **Biogeochemistry**, v. 79, n. 3, p. 361–382, jul. 2006.

BRADFORD, M. A. et al. Empirical evidence that soil carbon formation from plant inputs is positively related to microbial growth. **Biogeochemistry**, v. 113, n. 1–3, p. 271–281, 2013.

BRADLEY, R. Dynamics of nitrogen associated to acid insoluble substances derived from plant litter. **Communications in Soil Science and Plant Analysis**, v. 33, n. 7–8, p. 1277–1290, 2002.

BURDON, J. Are the traditional concepts the structures of humic substances realistic? **Soil Science**, v. 166, n. 11, p. 752–769, 2001.

CHAPUIS-LARDY, L.; CONTOUR-ANSEL, D.; BERNHARD-REVERSAT, F. High-performance liquid chromatography of water-soluble phenolics in leaf litter of three Eucalyptus hybrids (Congo). **Plant Science**, v. 163, n. 2, p. 217–222, 2002.

CHEN, R. et al. Soil C and N availability determine the priming effect: Microbial N mining and stoichiometric decomposition theories. **Global Change Biology**, v. 20, n. 7, p. 2356–2367, 2014.

CLARK, R. B. Characterization of phosphatase of intact maize roots. **Journal of agricultural and food chemistry**, v. 23, n. 3, p. 458–460, 1975.

COTRUFO, M. F. et al. The Microbial Efficiency-Matrix Stabilization (MEMS) framework integrates plant litter decomposition with soil organic matter stabilization: Do labile plant inputs form stable soil organic matter? **Global Change Biology**, v. 19, n. 4, p. 988–995, 2013.

COTRUFO, M. F. et al. Formation of soil organic matter via biochemical and physical pathways of litter mass loss. **Nature Geoscience**, v. 8, n. 10, p. 776–779, 2015.

CRAINE, J. M.; MORROW, C.; FIERER, N. Microbial nitrogen limitation increases decomposition. **Ecology**, v. 88, n. 8, p. 2105–2113, 2007.

DAVIDSON, E. A.; JANSSENS, I. A. Temperature sensitivity of soil carbon decomposition and feedbacks to climate change. **Nature**, v. 440, n. 7081, p. 165–173, 2006.

DENEF, K.; GALDO, I. Assessment of soil C and N stocks and fractions across 11 European soils under varying land uses. **Open Journal of Soil Science**, v. 3, n. November, p. 297–313, 2013.

DUNGAIT, J. A J. et al. Soil organic matter turnover is governed by accessibility not recalcitrance. **Global Change Biology**, v. 18, n. 6, p. 1781–1796, jun. 2012.

FONTAINE, S.; MARIOTTI, A.; ABBADIE, L. The priming effect of organic matter: A question of microbial competition? **Soil Biology and Biochemistry**, v. 35, n. 6, p. 837–843, 2003.

FREI, M. Lignin: Characterization of a multifaceted crop component. **The Scientific World Journal**, v. 2013, p. 1–25, 2013.

FULTON-SMITH, S.; COTRUFO, M. F. Pathways of soil organic matter formation from above and belowground inputs in a Sorghum bicolor bioenergy crop. **GCB Bioenergy**, v. 11, n. 8, p. 971–987, 2019.

GRANDY, A. S.; NEFF, J. C. Molecular C dynamics downstream: The biochemical decomposition sequence and its impact on soil organic matter structure and function. **Science of the Total Environment**, v. 404, n. 2–3, p. 297–307, 2008.

HADDIX, M. L.; PAUL, E. A.; COTRUFO, M. F. Dual, differential isotope labeling shows the preferential movement of labile plant constituents into mineral-bonded soil organic matter. **Global Change Biology**, v. 22, n. 6, p. 2301–2312, 2016.

HATCHER, P. G. et al. Comparison of two thermochemolytic methods for the analysis of lignin in decomposing gymnosperm wood: the CuO oxidation method and the method of thermochemolysis with tetramethylammonium hydroxide (TMAH). **Organic Geochemistry**, v. 23, n. 10, p. 881–888, 1995.

HEDGES, J. I.; KEIL, R. G. Organic geochemical perspectives on estuarine processes: sorption reactions and consequences. **Marine Chemistry**, v. 65, n. 1–2, p. 55–65, maio 1999.

HICKS PRIES, C. E. et al. Long term decomposition: the influence of litter type and soil horizon on retention of plant carbon and nitrogen in soils. **Biogeochemistry**, v. 134, n. 1–2, p. 5–16, 2017.

HILLI, S. et al. What is the composition of AIR? Pyrolysis-GC-MS characterization of acid-insoluble residue from fresh litter and organic horizons under boreal forests in southern Finland. **Geoderma**, v. 179–180, p. 63–72, 2012.

HOFFMANN, B. et al. Abundance and distribution of leaf wax n-alkanes in leaves of Acacia and Eucalyptus trees along a strong humidity gradient in northern Australia. **Organic Geochemistry**, v. 62, p. 62–67, set. 2013.

HUANG, W. et al. Trade-offs in soil carbon protection mechanisms under aerobic and anaerobic conditions. **Global Change Biology**, v. 26, n. 6, p. 3726–3737, 2020.

IUSS WORKING GROUP WRB. **World reference base for soil resources 2014. International soil classification system for naming soils and creating legends for soil maps**. [s.l: s.n.].

JACKSON, R. B. et al. The Ecology of Soil Carbon: Pools, Vulnerabilities, and Biotic and Abiotic Controls. **Annual Review of Ecology, Evolution, and Systematics**, v. 48, n. 1, p. 419–445, 2017.

JILLING, A. et al. Minerals in the rhizosphere: overlooked mediators of soil nitrogen

availability to plants and microbes. **Biogeochemistry**, v. 139, n. 2, p. 103–122, 2018.

KALLENBACH, C. M.; FREY, S. D.; GRANDY, A. S. Direct evidence for microbial-derived soil organic matter formation and its ecophysiological controls. **Nature Communications**, v. 7, p. 1–10, 2016.

KEILUWEIT, M. et al. Are oxygen limitations under recognized regulators of organic carbon turnover in upland soils? **Biogeochemistry**, v. 127, n. 2–3, p. 157–171, 22 fev. 2016.

KLEBER, M. What is recalcitrant soil organic matter? **Environmental Chemistry**, v. 7, n. 4, p. 320–332, 2010.

KLEBER, M. et al. **Mineral-Organic Associations: Formation, Properties, and Relevance in Soil Environments**. [s.l.] Elsevier Ltd, 2015. v. 130

KLEBER, M.; SOLLINS, P.; SUTTON, R. A conceptual model of organo-mineral interactions in soils: self-assembly of organic molecular fragments into zonal structures on mineral surfaces. **Biogeochemistry**, v. 85, n. 1, p. 9–24, jun. 2007.

KLOTZBÜCHER, T. et al. A study of lignin degradation in leaf and needle litter using 13C-labelled tetramethylammonium hydroxide (TMAH) thermochemolysis: Comparison with CuO oxidation and van Soest methods. **Organic Geochemistry**, v. 42, n. 10, p. 1271–1278, nov. 2011.

KNIGHT, T. G.; WALLWORK, M. A. B.; SEDGLEY, M. Leaf epicuticular wax and cuticle ultrastructure of four Eucalyptus species and their hybrids. **International Journal of Plant Sciences**, v. 165, n. 1, p. 27–36, jan. 2004.

KÖGEL-KNABNER, I. The macromolecular organic composition of plant and microbial residues as inputs to soil organic matter. **Soil Biology and Biochemistry**, v. 34, n. 2, p. 139–162, fev. 2002.

KÖGEL-KNABNER, I.; RUMPEL, C. Advances in molecular approaches for understanding soil organic matter composition, origin, and turnover: A historical overview. In: **Advances in Agronomy**. 1. ed. [s.l.] Elsevier Inc., 2018. p. 1–48.

KOLATTUKUDY, P. E. Structure, biosynthesis, and biodegradation of cutin and suberin. **Annual Review of Plant Physiology**, v. 32, n. 1, p. 539–567, jun. 1981.

KOPITTKE, P. M. et al. Nitrogen-rich microbial products provide new organo-mineral interactions for the stabilization of soil organic matter. **Global Change Biology**, n. July, p. 1–9, 2017.

KOPITTKE, P. M. et al. Nitrogen-rich microbial products provide new organo-mineral associations for the stabilization of soil organic matter. **Global Change Biology**, v. 24, n. 4, p. 1762–1770, abr. 2018.

KOPITTKE, P. M. et al. Soil organic matter is stabilized by organo-mineral associations through two key processes: The role of the carbon to nitrogen ratio. **Geoderma**, v. 357, n. June 2019, p. 113974, 2020.

KUZYAKOV, Y.; FRIEDEL, J. K.; STAHR, K. Review of mechanisms and quantification of priming effects. **Soil Biology and Biochemistry**, v. 32, n. 11–12, p. 1485–1498, 2000.

LAJTHA, K. et al. The detrital input and removal treatment (DIRT) network: Insights into soil carbon stabilization. **Science of The Total Environment**, v. 640–641, n. June, p. 1112–1120, 2018.

LAL, R. Forest soils and carbon sequestration. **Forest Ecology and Management**, v. 220, n. 1–3, p. 242–258, 2005.

LAROWE, D. E.; VAN CAPPELLEN, P. Degradation of natural organic matter: A thermodynamic analysis. **Geochimica et Cosmochimica Acta**, v. 75, n. 8, p. 2030–2042, 2011.

LAVALLEE, J. M. et al. Incorporation of shoot versus root-derived 13 C and 15 N into mineral-associated organic matter fractions: results of a soil slurry incubation with dual-labelled plant material. **Biogeochemistry**, v. 137, n. 3, p. 379–393, 2018.

LEHMANN, J. et al. Persistence of soil organic carbon caused by functional complexity. **Nature Geoscience**, jul. 2020.

LEHMANN, J.; KLEBER, M. The contentious nature of soil organic matter. **Nature**, v. 528, n. 7580, p. 60–68, 2015.

LIANG, C. et al. Quantitative assessment of microbial necromass contribution to soil organic matter. **Global Change Biology**, n. September, 2019.

LIANG, C.; SCHIMEL, J. P.; JASTROW, J. D. The importance of anabolism in microbial control over soil carbon storage. **Nature Microbiology**, v. 2, n. 8, 2017.

LIEBMANN, P. et al. Relevance of aboveground litter for soil organic matter formation – a soil profile perspective. **Biogeosciences Discussions**, n. January, p. 1–29, 2020.

LIM, CHIN HUAT & JACKSON, M. Dissolution for Total Elemental Analysis. In: **METHODS OF SOIL ANALYSIS Part 2, Second Edition**. [s.l: s.n.]. p. 1–12.

LYU, M. et al. Litter quality and site characteristics interact to affect the response of priming effect to temperature in subtropical forests. **Functional Ecology**, v. 33, n. 11, p. 2226–2238, 2019.

MALIK, A. A. et al. Soil microbial communities with greater investment in resource acquisition have lower growth yield. **Soil Biology and Biochemistry**, v. 132, n. November 2018, p. 36–39, maio 2019.

MARSCHNER, B. et al. How relevant is recalcitrance for the stabilization of organic matter in soils? **Journal of Plant Nutrition and Soil Science**, v. 171, n. 1, p. 91–110, 2008.

MELILLO, J. M. et al. Nitrogen and Lignin Control of Hardwood Leaf Litter Decomposition Dynamics. v. 63, n. 3, p. 621–626, 1982.

MILCU, A. et al. Identification of General Patterns of Nutrient and Labile Carbon Control on Soil Carbon Dynamics Across a Successional Gradient. **Ecosystems**, v. 14, n. 5, p. 710–719, 2011.

MWAFULIRWA, L. et al. Ryegrass root and shoot residues differentially affect short-term priming of soil organic matter and net soil C-balance. **European Journal of Soil Biology**, v. 93, n. January, p. 103096, 2019.

NELSON, P. N.; BALDOCK, J. A. Estimating the molecular composition of a diverse range of natural organic materials from solid-state 13 C NMR and elemental analyses. **Biogeochemistry**, v. 72, n. 1, p. 1–34, 2005.

NORTH, P. F. Towards an absolute measurement of soil structural stability using ultrasound. **Journal of Soil Science**, v. 27, n. 4, p. 451–459, 1976.

OSAWA, T.; NAMIKI, M. Natural antioxidants isolated from Eucalyptus leaf waxes.

Journal of Agricultural and Food Chemistry, v. 33, n. 5, p. 777–780, set. 1985.

OSONO, T.; TAKEDA, H.; AZUMA, J. I. Carbon isotope dynamics during leaf litter decomposition with reference to lignin fractions. **Ecological Research**, v. 23, n. 1, p. 51–55, 2008.

PRESTON, C. M.; NAULT, J. R.; TROFYMOW, J. A. Chemical changes during 6 years of decomposition of 11 litters in some Canadian forest sites. Part 2. 13C abundance, solid-state 13C NMR spectroscopy and the meaning of “lignin”. **Ecosystems**, v. 12, n. 7, p. 1078–1102, 2009.

PRESTON, C. M.; TROFYMOW, J. A. Variability in litter quality and its relationship to litter decay in Canadian forests. **Canadian Journal of Botany**, v. 78, n. 10, p. 1269–1287, 2000.

PRESTON, C. M.; TROFYMOW, J. A. The chemistry of some foliar litters and their sequential proximate analysis fractions. **Biogeochemistry**, v. 126, n. 1–2, p. 197–209, 2015.

RAMIN, K. I.; ALLISON, S. D. Bacterial tradeoffs in growth rate and extracellular enzymes. **Frontiers in Microbiology**, v. 10, n. December, p. 1–10, dez. 2019.

RASSE, D. P.; RUMPEL, C.; DIGNAC, M.-F. Is soil carbon mostly root carbon? Mechanisms for a specific stabilisation. **Plant and Soil**, v. 269, n. 1–2, p. 341–356, fev. 2005.

RYAN, M. G.; MELILLO, J. M.; RICCA, A. A comparison of methods for determining proximate carbon fractions of forest litter. **Canadian journal of Forest Research**, n. 20, p. 166–171, 1990.

SANTOS, S. A. O. et al. Characterization of phenolic components in polar extracts of Eucalyptus globulus Labill. bark by high-performance liquid chromatography–mass spectrometry. **Journal of Agricultural and Food Chemistry**, v. 59, n. 17, p. 9386–9393, set. 2011.

SCHMIDT, M. W. I. et al. Persistence of soil organic matter as an ecosystem property. **Nature**, v. 478, n. 7367, p. 49–56, 5 out. 2011.

SHAHBAZ, M. et al. Microbial decomposition of soil organic matter is mediated by quality and quantity of crop residues: mechanisms and thresholds. **Biology and Fertility of Soils**, v. 53, n. 3, p. 287–301, 2017.

SHI, A.; PENFOLD, C.; MARSCHNER, P. Decomposition of roots and shoots of perennial grasses and annual barley-separately or in two residue mixes. **Biology and Fertility of Soils**, v. 49, n. 6, p. 673–680, 2013.

SJÖBERG, G. et al. Degradation of hemicellulose, cellulose and lignin in decomposing spruce needle litter in relation to N. **Soil Biology and Biochemistry**, v. 36, n. 11, p. 1761–1768, 2004.

SLUITER, J. B. et al. Compositional analysis of lignocellulosic feedstocks. 1. Review and description of methods. **Journal of Agricultural and Food Chemistry**, v. 58, n. 16, p. 9043–9053, ago. 2010.

STEWART, C. E. et al. Soil carbon saturation: Implications for measurable carbon pool dynamics in long-term incubations. **Soil Biology and Biochemistry**, v. 41, n. 2, p. 357–366, 2009.

VERSINI, A. et al. Nitrogen dynamics within and between decomposing leaves, bark

and branches in Eucalyptus planted forests. **Soil Biology and Biochemistry**, v. 101, p. 55–64, 2016.

VON LÜTZOW, M. et al. Stabilization of organic matter in temperate soils: mechanisms and their relevance under different soil conditions - a review. **European Journal of Soil Science**, v. 57, n. 4, p. 426–445, ago. 2006.

XIAO, C. et al. Priming of soil organic matter decomposition scales linearly with microbial biomass response to litter input in steppe vegetation. **Oikos**, v. 124, n. 5, p. 649–657, 2015.

ZECH, W. et al. CPMAS 13C NMR and IR spectra of spruce and pine litter and of the Klason lignin fraction at different stages of decomposition. **Zeitschrift für Pflanzenernährung und Bodenkunde**, v. 150, n. 4, p. 262–265, 1987.

2.8. Supplementary information

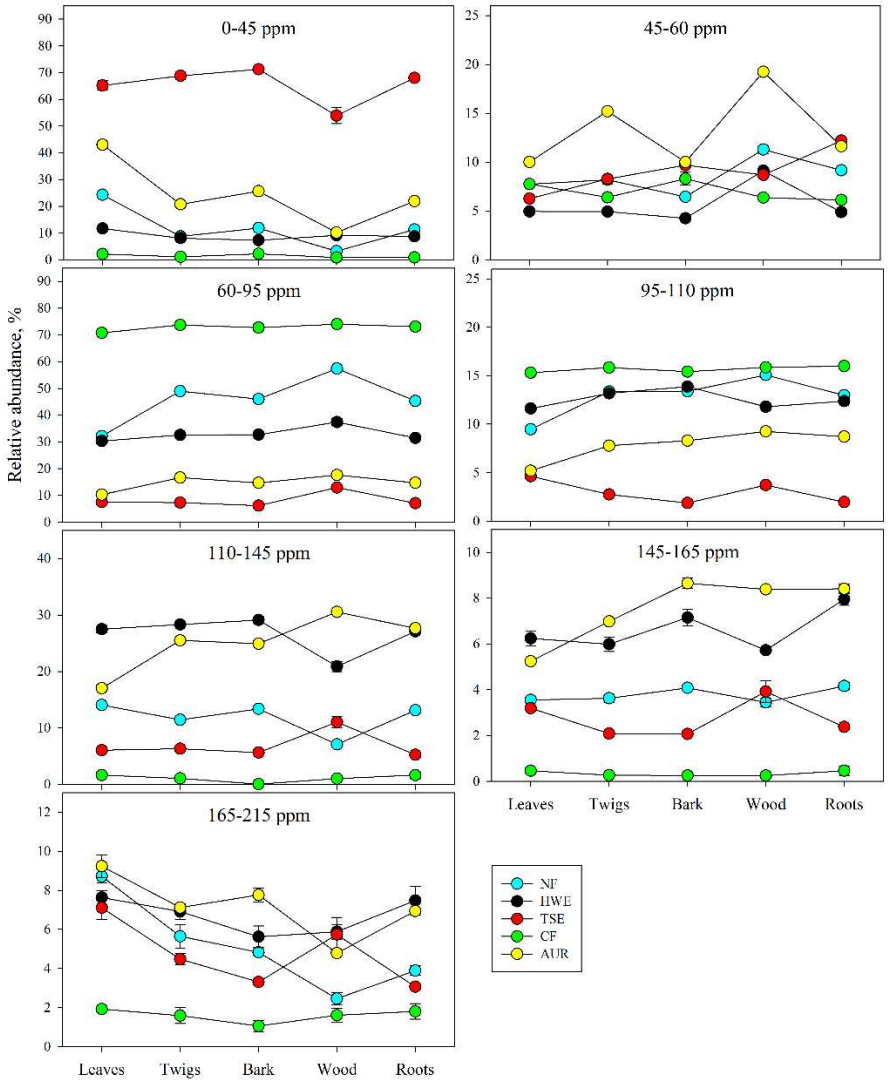

Supplementary Fig. 1. Relative abundance of Alkyl C (0–45 ppm); N-Alkyl/Methoxyl-C (45–60 ppm); O-Alkyl C (60–95 ppm); Di-O-Alkyl C (95–110 ppm), Aromatic C (110–145 ppm); Phenolic-C (145–165 ppm); and Amide/Carboxylic-C (165–215 ppm). The data set was obtained from non-fractionated (NF) plant organs and their biochemical fractions namely, hot water extractables (HWE), total solvent extractables (TSE), cellulosic fraction (CF), and acid unhydrolyzable residue (AUR) using solid-state ^{13}C cross-polarization magic angle spinning (CPMAS) NMR spectroscopy.

3. CHAPTER II – FOREST LITTER CONSTRAINTS ON THE PATHWAYS CONTROLLING SOIL ORGANIC MATTER FORMATION

3.1. Abstract

Although forests have a significant ecological relevance for soil C pools, the connection between litter chemistry and the pathways controlling soil organic matter (SOM) formation in forest ecosystems remains poorly understood. We addressed this question by incubating samples of a Ferralsol for 200 days with typical forest litter (leaves, twigs, bark and roots) obtained from ^{13}C-enriched *Eucalyptus* seedlings. Throughout the incubation, we monitored $^{13}C/^{12}C–CO_2$ evolved from the soil to quantify the microbial respiration of the ^{13}C-labeled fresh plant litter and of the "native" SOM. Afterwards, we used density fractionation to obtain particulate organic matter (POM) with density <1.8 g cm^{-3}, and the soil material remaining was wet-sieved to obtain SOM with particle-size >53 µm and mineral-associated SOM (MAOM, with particle-size <53 µm). The molecular composition of plant material and SOM fractions was determined by solid-state ^{13}C-CPMAS-NMR spectroscopy. Microbial amino sugars were quantified in bulk soil using gas chromatography. Our $^{13}C/^{12}C–CO_2$ results indicate that leaves, twigs and bark (aboveground litter) were respired at higher rates but led to lower degradation of "native" SOM as compared to root tissues. In average, aboveground litter promoted net C gains in both POM and MAOM, whereas root litter only led to net C gains in POM. Generally, SOM formation via microbial incorporation of aboveground litter through *in vivo* pathways appears to be more efficient and causes less degradation of "native" MAOM than roots. Moreover, a reduction in microbial amino sugars in bulk soils suggests that *in vivo* pathways also favored the formation of POM, which had more microbial-derived proteins than forest litter. Overall, modeling the connection between litter chemistry and the pathways controlling SOM formation should include a framework that considers the mineralization of "native" SOM and the vertical separation of aboveground and belowground C inputs in forest ecosystems.

Keywords: Plant tissue biochemistry. Hot water extractables. In vivo pathway. Priming effect. ^{13}C-CP/MAS-NMR spectroscopy. Tropical soils. Root litter. Particulate organic matter. Mineral-associated organic matter.

3.2. Introduction

Forest soils are an important component of the global terrestrial C pool, but significant knowledge gaps exist for the pathways controlling the formation of soil organic matter (SOM) from different plant residues in these ecosystems. Historically, “recalcitrant” constituents of plant litter were thought to be selectively preserved as SOM, while “labile” materials would be preferentially respired to CO_2 by soil microorganisms (MELILLO et al., 1982). Paradoxically, an emerging view suggests that “labile” constituents of plant litter are in fact incorporated into SOM by microorganisms (COTRUFO et al., 2015), and subsequently retained as mineral-associated SOM (KOPITTKE et al., 2018, 2020). Yet, Cotrufo *et al.* (2015) also argue that because microorganisms are less efficient in assimilating “recalcitrant” components of plant litter, these materials can be selectively preserved in SOM. In this case, such *ex vivo* pathways (e.g., selective preservation) are more important than their *in vivo* (i.e. microbial incorporation) counterparts (LIANG; SCHIMEL; JASTROW, 2017). Nonetheless, some specific traits of forest ecosystems need to be considered in light of these emerging paradigms. Firstly, forest litter includes a range of materials (e.g., leaves, twigs, branches and roots), which incorporation into SOM should depend on both *in vivo* and *ex vivo* pathways (LIANG; SCHIMEL; JASTROW, 2017). Secondly, the control of litter chemistry on SOM formation is often masked by different plant litter inputs into soils above and belowground, especially in forest ecosystems. Last but not least, the degradation of “native” SOM driven by fresh plant litter inputs due to priming effects cannot be overlooked as well. Therefore, addressing these issues is critical to improve our knowledge on C dynamics in forest soils, linking plant residue processing to the sequestered SOM.

The specific pathways through which “labile” and “recalcitrant” materials are incorporated into SOM ultimately depend on the interaction between substrate chemistry and microorganisms. Plant material enriched in easily degradable compounds such as leaf litter (e.g., high content of soluble constituents, low C:N ratio) are more likely to be incorporated by microorganisms (*in vivo* pathway), which cell constituents and/or by products are subsequently transferred into SOM, especially to mineral-associated organic matter (MAOM) (COTRUFO et al., 2013; KOPITTKE et al., 2020; LIANG et al., 2019; LIANG; SCHIMEL; JASTROW, 2017). Otherwise, for plant

material enriched in less degradable components as typically observed in roots (e.g., high hydrophobicity, wide C:N ratio), *ex vivo* pathways also can play a significant role in SOM formation. Indeed, this pathway appears to be particularly important for the accumulation of plant debris as particulate organic matter (POM) (ANGST et al., 2019; COTRUFO et al., 2015; HADDIX; PAUL; COTRUFO, 2016). However, there is uncertainty on whether *in vivo* and *ex vivo* pathways are more impacted by temporal or spatial constraints in soils. As such, some authors argue that POM is formed first but it is continuously processed by microorganisms and transferred into MAOM (LEHMANN; KLEBER, 2015). Other authors instead, claim that POM and MAOM are formed in divergent, but simultaneous pathways (COTRUFO et al., 2015; FULTON-SMITH; COTRUFO, 2019; HADDIX; PAUL; COTRUFO, 2016). Either way, considerations to such constraints on the pathways controlling SOM dynamics should be proportionally more important in forest soils. This is because C inputs above and belowground exhibit strong spatiotemporal variations in forest soils, hence adding significant uncertainty to our understanding on SOM formation and decay in these ecosystems.

Many studies have shown that the addition of fresh substrates stimulates the decomposition of “native” soil C in a process often referred to as “priming effect” (FONTAINE; MARIOTTI; ABBADIE, 2003; KUZYAKOV; FRIEDEL; STAHR, 2000). However, such “priming effect” is often neglected in studies aiming to connect litter chemistry and SOM formation. Part of this is because the relationship between litter chemistry (e.g., above and belowground litter) and the resulting “native” SOC mineralization is not straightforward (CHEN et al., 2014; FONTAINE; MARIOTTI; ABBADIE, 2003; KUZYAKOV; FRIEDEL; STAHR, 2000; LYU et al., 2019). Moreover, such “priming effect” involves complex processes that depend not only on the properties of litter inputs or “native” SOM, but also on nutrient availability in the system, shifts in microbial communities (CRAINE; MORROW; FIERER, 2007; MILCU et al., 2011). Owing to its simultaneous dependence on several factors, even studies on the “priming effect” with comparable soils incubated with similar plant materials (e.g., grass litter) conducted under controlled conditions can exhibit very different results. For instance, Mwafulirwa *et al.* (2019) reported that shoot litter caused higher mineralization of “native” SOM than root material, whereas Shahbaz *et al.* (2017) observed that grass root inputs resulted in comparatively higher mineralization of

"native" SOM than shoot material. If we consider that grass litter (mostly roots, straw and leaves) is comparatively more uniform than forest litter (leaves, roots, twigs, barks, and coarse wood debris), the "priming" of "native" SOM should be more complex in the latter. These aspects also highlight the importance of determining how and to what extent the formation of SOM via *in vivo* and *ex vivo* pathways is linked to litter chemistry and the mineralization of "native" SOM.

In the present study we aimed to disentangle how the chemical composition of forest litter types determines the formation of specific SOM pools along with the mineralization of "native" SOM. To this end, we incubated ^{13}C enriched *Eucalyptus spp.* aboveground litter (leaves, twigs and bark) and roots in soil samples for 200 days. During this period, we monitored the respiration of the ^{13}C-labeled litter and quantified the release of CO_2 from the "native" SOM. This allowed us to determine the extent to which the respiration of the "native" SOM varied as a function of litter chemistry. At the end of the experiment, we quantified the C incorporation of litter-C into SOM fractions. Further, we inferred the molecular chemistry of these fractions using solid-state ^{13}C-CPMAS-NMR spectroscopy and determined the contribution of microbial amino sugars to SOM in bulk soil using gas chromatography.

3.3. Materials and methods

3.3.1. Soil and plant material used for incubation experiment

The soil used in the incubation was collected from the topsoil layer (0–20 cm) of a sandy-loam Haplic Ferralsol (IUSS Working Group WRB, 2014) at Paula Candido, Minas Gerais – Brazil (20º 52' S, 42º 58' E). After sampling, the soil material collected was air dried, sieved through a 2.0 mm screen, and stored for characterization, which was based on chemical, physical and mineralogical analysis. As such, chemical analyses indicated that the soil had a pH of 5.7 in H_2O and 4.6 in KCl; Ca^{2+} and Mg^{2+} contents were 1.8 and 1.2 $cmol_c\ dm^{-3}$, respectively (extraction with KCl 1 mol L^{-1}); P and K contents were 3.60 and 85.0 mg dm^{-3}, respectively (extracted by Mehlich-1: HCl 0.05 mol L^{-1} + H_2SO_4 0.025 mol L^{-1}). Based on particle-size determination, the sand-sized fraction represented 52 % of soil total mass (as determined by wet sieving), whereas clay- and silt-sized particles contents were about 31 and 17 %, respectively

(determined by the pipette method). According to a thermal analysis procedure, kaolinite was the predominant mineral in the clay fraction (220 g kg^{-1} soil), and the original soil organic carbon (SOC) content was 27.0 g kg^{-1} soil and the $\delta^{13}C_{VPDB}$ = –16 ‰. Moreover, the soil had a water holding capacity (WHC) of 0.2 g g^{-1} soil.

The eucalypt plant organs used in the present study (i.e. leaves, twigs, bark and roots) were labeled with ^{13}C as described in Almeida et al. (2018). Briefly, two-months old seedlings of a eucalypt hybrid (*Eucalyptus grandis* × *Eucalyptus urophylla*) were grown in a chamber supplemented with Clark nutrient solution (CLARK, 1975). After the isotopic labeling (conducted over 126 days), the seedlings were harvested and fractionated into leaves, twigs, bark and roots. Subsequently, the plant organs were dried under a forced-draft oven at 60 °C and ground separately on a Wiley mill. Total C content and the relative abundance of ^{13}C ($\delta^{13}C$) in each plant organ were determined in an isotope ratio mass spectrometer- IRMS (ANCA-GSL, 20-20, Sercon, Crewe-UK) (Supplementary table 1). Additionally, subsamples of the milled plant organs were digested with a mixture of nitric and perchloric acid (4:1, v/v) and their nutrient contents were determined by inductively coupled plasma optical emission spectrometry (ICP-OES, Varian Vista-Pro CCD Simultaneous ICP-OES) (Supplementary table 2). Additionally, we determined the contents of extractables and structural compounds determined four plant organs (leaves, twigs, bark and roots) within four operationally defined “biochemical fractions”, namely: HWE-hot water extractables (often referred to as ‘metabolic’ compounds); TSE-total solvent extractables (free lipids), CF-cellulosic fraction (mostly cellulose and hemicellulose), and AUR- acid unhydrolyzable residue (mostly lignin, lipids, and proteins) as described in Almeida *et al.*(2018). Briefly, the HWE fraction was obtained by extracting each plant organ with deionized for 6 h and the residue generated after the HWE extraction was treated with acetone for 6 h to obtain the TSE fraction. Both HWE and TSE were submitted to a continuous reflux in Soxhlet extractors. Subsequently, the residue free of HWE and TSE was split in two parts, and the CF and AUR were obtained in separated procedures. Hence, half of residue free from extractables was treated with a mixture of ethanol and aqueous HNO_3 (65 %, v/v) at a ratio of 4:1 for 1 h (extraction repeated four times) and then with an aqueous solution of KOH 25 % (m/v) for 1 h to obtain the CF. From the other half, we isolated the AUR fraction, by treating the material with concentrated H_2SO_4 (72 %, v/v) for 1 h and subsequently with aqueous

H_2SO_4 (3 %, v/v) for 4 h. All the biochemical fractions obtained were freeze-dried and had their dry mass yield determined (Fig. 1).

3.3.2. Incubation experiment and gases monitoring

For the incubation, the experiment included a control treatment (soil only) and four treatments with the addition of each ^{13}C-labeled plant organ (leaves, twigs, bark and roots) placed in separate microcosms. In total, we had 15 microcosms (experimental units) disposed in a completely randomized block design with three replicates for each treatment. Plant litter additions were fixed at a proportion of 10 mg C g^{-1} soil, thoroughly mixed with 20 g of air-dried soil and placed into 0.57 L air-tight glass jars with rubber septa in their lids to allow headspace gas sampling. The samples remained incubated for 200 days a moisture content fixed at 80 % of their WHC under controlled temperature (25 ± 2 ºC). In order to guarantee the presence of a comparable microbial community commonly found in forest environments, all samples were inoculated with a suspension (5:1 water:soil ratio) of fresh soil collected from a soil cultivated with eucalyptus plants. The inoculation consisted on applying 100 µL of the suspension in all experimental units. Over the incubation period, soil respiration was assessed on days 1, 2, 3, 4, 7, 10, 13, 21, 28, 38, 46, 70, 80, 92, 112, 148, 178 and 200 days after the experiment began. After each sampling, the jars were completely vented with a small fan and remained tightly closed until the next assessment. This procedure was used to promote gas exchange and prevent anoxic condition inside the jars between subsequent samplings.

3.3.3. Soil fractionation based on density and particle size

At the end of the incubation experiment (200 days), soil subsamples were taken, air-dried and submitted to a physical fractionation using a combination of density- and particle-size separation (ALMEIDA et al., 2018; DENEF; GALDO, 2013). Firstly, we used the density fractionation to isolate particulate organic matter (POM), by placing 5g of the air-dried soil into a 100 mL of sodium polytungstate (SPT) solution with a density of 1.80 g cm^{-3} and dispersing the soil with a calibrated probe-tip sonicator (NORTH, 1976), at 800 J mL^{-1}. Afterwards, the samples were centrifuged and the floating POM (free and occluded fractions) which contains mainly plant derived

material was collected in a 0.22 µm pore nylon filter coupled to a pressure filtration system. To reverse clay flocculation caused by centrifugation of mineral fraction, the samples were submitted to a second sonication 100 mL of deionized water. Subsequently, the heavy mineral fraction (density > 1.80 g cm^{-3}) was wet sieved through a 53 µm screen to obtain the fractions smaller than 53 µm (MAOM) and greater than 53 µm (sand-sized). It turns out that the sand-sized SOM represented only a small proportion of total SOM (1%) and it is probably an operational artefact caused by the lack of a 100 % removal of POM from sand. The SPT solution remaining within the POM and MAOM fractions was removed by extensively rinsing the soil materials with deionized water using a high-pressure filtration unit until an electrical conductivity (EC) lower than 5 µS cm^{-1} was reached. After the complete removal of salts, the samples were freeze dried and stored for further analyses.

3.3.4. Isotope content and C partitioning

Throughout the incubation, we quantified the C-CO_2 evolved from the microcosms and used ^{13}C data to trace its sources (native SOM or ^{13}C-enriched plant organ types). During each sampling, we collected a 100-mL aliquot of air from the headspace of each jar and the $^{13}C/^{12}C–CO_2$ concentrations were analyzed using a cavity ring-down spectrometer (CRDS, G2131-i, Picarro, Sunnyvale, CA). In addition, we used ^{13}C data to follow the incorporation of litter-derived C into each fraction of SOM obtained in the physical fractionation. As such, total content of C and the relative abundance of ^{13}C ($\delta\ ^{13}C$) of each SOM fraction were determined in an isotope ratio mass spectrometer- IRMS (described above). Subsequently, the contribution of litter derived-C for total soil respiration and for each SOM fraction was determined using a two-end member isotope mixing model (STEWART et al., 2009):

$f_{po} = (\delta t – \delta s)/(\delta r – \delta s)$

where:

f_{po} = the proportion of a given plant organ derived-C in a given SOM fraction or total CO_2 evolved.

$\delta t = \delta^{13}C$ of a given SOM fraction or CO_2 of the treatment with a specific plant organ;

δs = $\delta^{13}C$ of the SOM fraction or the CO_2 of the treatment without litter addition (soil only);

δr = $\delta^{13}C$ of the labeled plant organ used in this study (Supplementary Table 1).

3.3.5. Microbial biomarkers analysis

In order to quantify the contribution of microbial necromass to SOM formation we evaluated the variation in microbial biomarkers as a function of the different litter types used in the incubation. To this end, we extracted glucosamine, mannosamine, galactosamine, and muramic acid from bulk soil samples according to the methodology described by Zhang and Amelung (1996) and Liang et al. (2012). Accordingly, 400 mg soil subsamples were finely ground and hydrolyzed with 10 mL of a HCl solution at 6 mol L–1 at 105 °C for 8 h. Then, the hydrolysate was filtered, and the filtrate was completely dried in a rotary evaporator at 40 ºC under vacuum. Afterwards, the residue was purified through neutralization with a KOH solution at 0.4 mol L–1 and salt precipitation in methanol and deionized water. After these steps, the samples were derivatized to aldonitrile acetates using 32 mg mL^{-1} hydroxylamine hydrochloride and 40 mg mL–1 4-(dimethylamino) pyridine in pyridine-methanol (4:1, v/v) solutions. Subsequently, the dried extracts were then redissolved in a mixture of ethyl acetate and hexane (1:1, v:v) and the measurements performed on a Trace 1300 gas chromatograph (GC) (Thermo Fisher Scientific) equipped with a ZB–5HT column (60 m length, 0.25 I.D., 0.25 µm film thickness; Phenomenex LTD, Aschaffenburg, Germany) and a flame ionization detector. Myo-inositol was utilized as an internal standard and the GC oven temperature configurations used in the present analysis were the same presented by Angst et al.(2018) as follows: the initial temperature was set at 120 °C and held constant for 4 min. Subsequently, the temperature was increased to 250 °C at 30 °C min–1 and held constant for 10 min. For the next stage, the target temperature was 280 °C at 5 °C min–1 held constant for 10 min. In the final stage, the samples were heated to 320 °C at 30 °C min–1 held constant for 10 min. The sample injection was made in split mode (1:10) with an injector temperature of 260 °C and the ultrapure He was the carrier gas at a constant flow rate of 1 mL min–1. All amino sugars were quantified through the application of calibration curves derived from

an external standard based on different concentrations of target analytes and normalized to the GC response factor that was always close to 1. The concentrations of the analytes of interest were normalized to the SOC content of the respective sample. Bacterial and fungal necromass were estimated based in the amino sugar content in soil according to Liang et al. (2019).

3.3.6. Characterization of plant material and SOM factions using NMR spectroscopy

The molecular composition of the plant material and SOM fractions, that is, POM and MAOM were characterized using solid-state ^{13}C cross-polarization magic angle spinning (CPMAS) NMR spectroscopy (Bruker DSX 200 spectrometer, Bruker BioSpin GmbH). All samples were filled into a zirconium dioxide rotor and the measurements conducted at a rotation speed of 6.8 kHz, with a 'magic angle' around 54.74 ° and an acquisition time of 0.01024 s. Delay times were adjusted to the different plant materials: 1.0 s for plant material and POM, and 0.8 s for the MAOM fraction. All spectra were subdivided into seven integration areas: 0–45 ppm (alkyl-C), 45–60 ppm (N-Alkyl/Methoxyl-C), 60–95 ppm (*O*-Alkyl-C), 95–110 ppm (Di-*O*-Alkyl-C), 110–145 ppm (Aromatic-C), 145–165 ppm (Phenolic-C) and 165–215 ppm (Amide/Carboxylic-C). These integration areas together with C and N contents of the samples analyzed were used to estimate the relative abundance of carbohydrate, protein, lignin, lipid, carbonyl and char (not considered for plant material) using the Molecular Mixing Model (NELSON; BALDOCK, 2005). We further referred to this method as NMR-MMM in this text.

3.3.7. Total digestion and elemental analysis

In order to determine the effect of litter amendments on the contents of diverse elements in soil, we submitted the samples to total digestion (Lim & Jackson, 1982). Approximately 100 mg of fine milled soil samples were weighed in platinum crucibles and treated with a mixture of aqueous solutions of perchloric ($HClO_4$) and nitric acid (HNO_3) at a 4:1 ratio. The concentration of each acid solution before the mixing was 60 % (v/v) for $HClO_4$ and 65 % (v/v) for HNO_3. The samples were heated until the temperature reached 150 °C on a sand-bath and held constant until SOM was

completely oxidized. Subsequently, the temperature was raised to 300 °C to vaporize the acids. After drying, the samples were treated with an aqueous hydrofluoric acid (HF) solution at 40 % (v/v) and left to cool overnight. In the following day, 4 mL of $HClO_4$ were added to the samples and heated up to 300 °C on a sand-bath to vaporize the acid. This procedure was repeated twice. Afterwards, 4 mL of an aqueous solution of HCl (37 %, v/v) were added and the samples heated to dissolve the material remaining from the digestion step. Finally, the digestion product had the volume completed to 50 mL, the solution was filtrated and its total content of aluminum (Al), calcium (Ca), iron (Fe), potassium (K), magnesium (Mg), manganese (Mn), sodium (Na), phosphorus (P) and Sulphur (S) was analyzed by inductively coupled plasma optical emission spectrometry (ICP-OES, Varian Vista-Pro CCD Simultaneous ICP-OES) (Supplementary table 3).

3.4. Results

3.4.1. Characterization of plant material used for incubation

According to our results, the C:N ratio of the plant material used in the incubation varied between 24 for leaves up to 76 for bark, with intermediary values observed for twigs (57) and roots (56) (Fig. 1A). In addition, our proximate analysis indicated significant variations in HWE, TSE, CF, and AUR content within each plant organ evaluated. As such, leaves presented highest contents of extractables in water (HWE) and acetone (TSE), and smallest amounts of structural components (CF and AUR) among all the plant organs evaluated (Fig. 1B). In contrast, roots showed significantly higher amounts of AUR and lower amounts of HWE as compared to the other plant components. Moreover, twigs and bark presented similar proportions of all biochemical fractions in their tissues, except for the comparatively lower amount of TSE in the former (Fig. 1 B). Additionally, the NMR-MMM results evidenced that leaves and roots showed the most contrasting chemical composition among all the plant organs evaluated. Leaves were more enriched in lipids and proteins and presented comparatively lower amounts of carbohydrates (Fig. 1C), whereas roots tended to be slightly richer in lignin and exhibited very low amounts of carbonyl groups. Twigs, bark and roots presented comparable contents of carbohydrates and proteins (Fig. 1C).

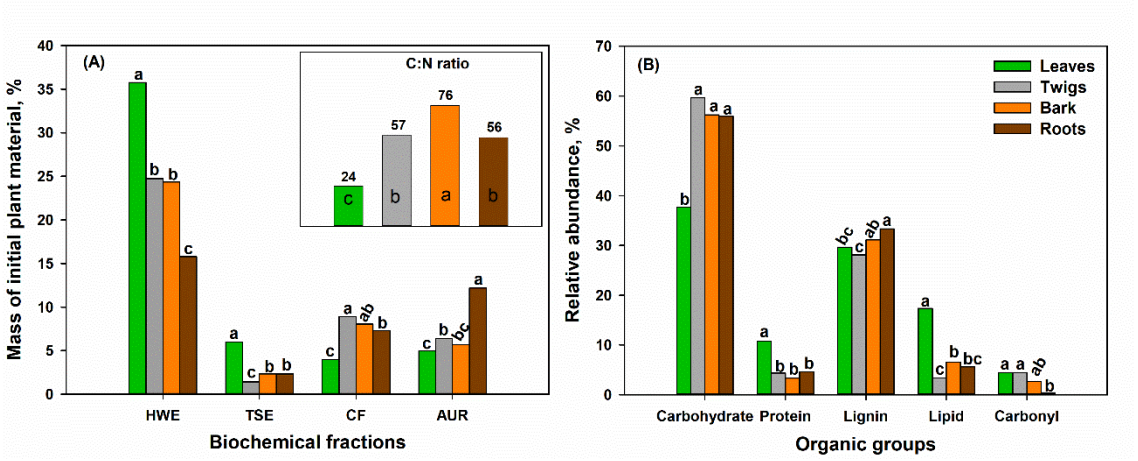

Fig. 1. Characterization of plant material based on proximate analysis, C:N ratio, and modelled compound classes based on ^{13}C-CPMAS NMR spectroscopy data combined with the Molecular Mixing Model (NELSON; BALDOCK, 2005); A) Partitioning of biochemical factions in leaves, twigs, bark and roots of eucalypt plants into hot water extractables (HWE), total solvent extractables (TSE), cellulosic fraction (CF) and acid unhydrolyzable residue (AUR); Bulk C:N ratio of leaves, twigs, bark and roots of eucalypt plants (inset); and B) Relative abundance of the main organic groups (carbohydrate, protein, lignin, lipid and carbonyl) within each plant organ evaluated. For a given organic group, biochemical fraction and plant organs, means followed by the same lowercase letter do not differ at $p<0.05$ (Tukey's test).

3.4.2. Soil respiration dynamics and C-CO2 partitioning

Our C-CO_2 data obtained throughout the incubation indicated the following order for the total soil respiration: controls < roots < bark < leaves < twigs (Fig. 3A). Total C-CO_2 evolution varied between 2.92 ± 0.02 for roots up to 3.57 ± 0.05 mg C g^{-1} soil in the samples treated with twigs. In comparison the cumulative C-CO_2 from the control accounted for 1.15 ± 0.02 mg C g^{-1} soil. Intermediate values occurred for leaves (3.42 ± 0.04 mg C g^{-1} soil), 3.20 ± 0.03 mg C g^{-1} soil for bark, and 2.92 ± 0.02 mg C g^{-1} soil for roots (Fig. 3B). After partitioning the total C-CO_2 between litter and "native" SOM some interesting trends emerged. Accordingly, soil samples treated with leaves showed the highest release of litter-C, which accounted for 67 % of the total C-CO_2, with only 33 % derived from the respiration of "native" SOM. Moreover, only in these samples the mineralization of the "native" SOM did not differ from the control treatment (Fig. 3B). In contrast, in soil samples incubated with roots, its contribution to the total C-CO_2 was only 49 %, with 51 % derived from "native" SOM. For twigs and bark, these materials accounted for 59 % and 61 % of total C-CO_2, with no significant differences

between them at $p<0.05$ (Fig. 3B). In these treatments the contribution of “native” SOM to total C-CO_2 was 41, and 39 %, respectively. In average, the release of C-CO_2 from “native” SOM in the presence of roots was approximately 13.3 % higher (absolute values) than the other plant organs evaluated.

When plotted over the entire period of the incubation, the contribution of plant litter and “native” SOM to total C-CO_2 emissions allowed us to compare these C sources directly (Fig. 3C-F). Generally, soil samples incubated with leaves, twigs and bark presented similar temporal respiration dynamics, with litter derived-C being respired predominantly at higher rates than “native” SOM during most of the incubation period (Fig. 3C-E). Apparently, these plant organs were rapidly incorporated and respired at higher rates as compared to the “native” SOM up to 150 days of incubation. Interestingly, there was no clear distinction between the respiration rate of roots and that of the “native” SOM for the entire period of incubation (Fig. 2F). In this case, both sources showed similar contributions to total C-CO_2 emissions. Irrespective of plant organ, the highest respiration rates of “native” SOM occurred in the first hours of incubation reaching up to 80 % of the total C-CO_2 emissions. Afterwards, the respiration of “native” SOM rapidly declined with a concomitant increase of litter derived-C respiration in all treatments, except for roots. Over the last 50 days of the incubation experiment, the relative contribution of litter-derived C and “native” SOM for total soil respiration tended to converge to approximately 50 %, with highest variability observed for root litter.

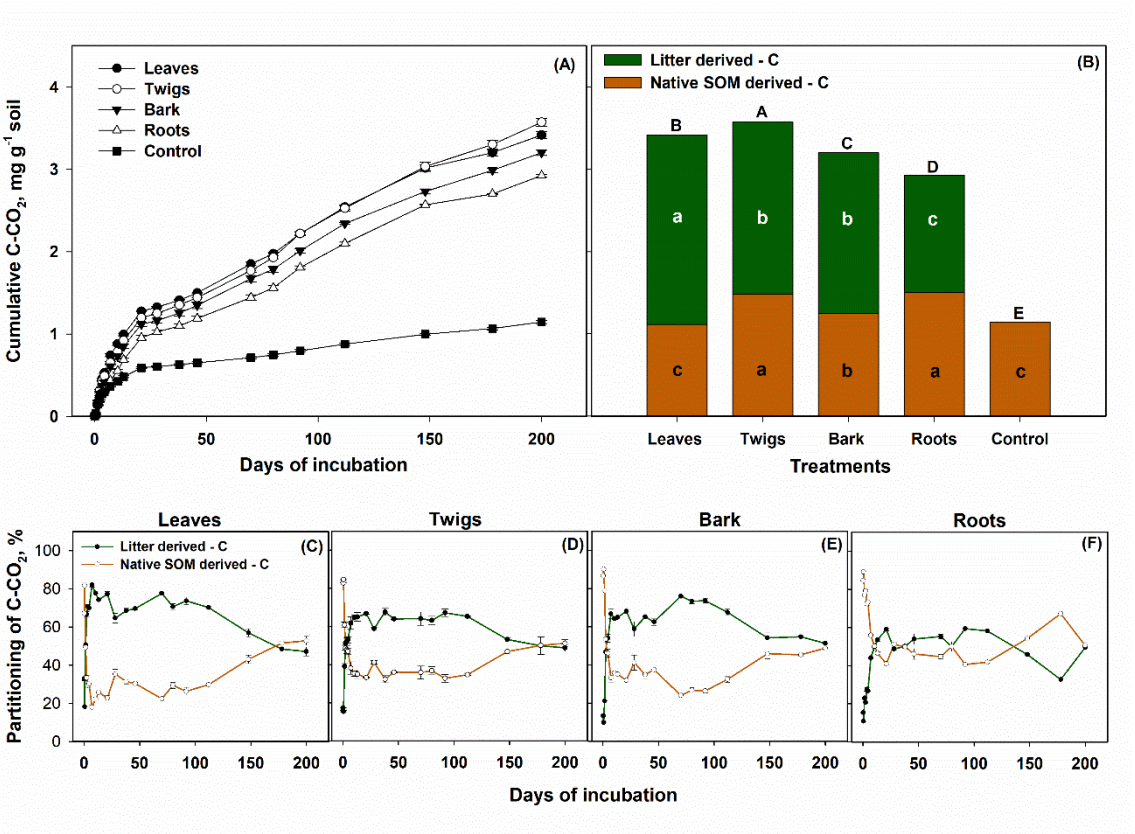

Fig. 2. Total soil respiration, and the partition of C-CO_2 from forest litter and "native" soil organic matter. A) Cumulative C-CO_2 evolved from soil samples incubated without plant litter (control) or amended with leaves, twigs, bark and roots of eucalyptus over 200 days; B) Partitioning of total (cumulative) C-CO_2 evolved throughout the incubation period and C–F) Variation in litter-derived and native soil organic matter derived C-CO_2 throughout the incubation experiment. Uppercase letters compare total CO_2 (litter + native SOM derived-C) and lowercase letters compare the C-CO_2 respired from a specific C pool. Means followed by the same letter do not differ among the treatments at $p<0.05$ (Tukey's test).

3.4.3. Total SOC content and its distribution among SOM fractions

Throughout the incubation, the control treatment showed a C loss that was approximately 12 % of the initial total soil C content, which was about 27.0 g kg^{-1} soil before the experiment had started. For the treatments with litter amendment, total soil C content increased in response to the addition of leaves and twigs (Fig. 3A), consistent with a recovery of 60 % and 55 % of litter-derived C in these respective treatments (Fig. 3B). In contrast, despite the high recovery rate of litter-derived C in the samples amended with bark (50 %) and roots (58 %) (Fig. 3B), there was not a significant increase in total soil C content in these treatments (Fig. 3A).

The distribution of total soil C content within SOM fractions in the non-amended soil samples before incubation was: 86 % within the MAOM and 12 % in the POM fraction. After the incubation, we observed a significant reduction in the C content stored within the MAOM fraction in the control treatment. Otherwise, no significant differences were detected in the soil C stored within the POM (Fig. 3A). For the treatments receiving plant litter, about 27 % of the initial C input was recovered in the MAOM, 27 % in the POM and only 1 % in the sand-sized fraction (Fig. 3B). Among all treatments receiving plant litter, only leaves resulted in significant increase in total C content within the MAOM fraction (Fig. 3A). For the samples treated with twigs and bark, there was a trend of increasing the C content in the MAOM, whereas in the samples incubated with roots the MAOM-C remained similar to the initial soil (Fig. 3A). Moreover, roots transferred more C into the POM (38 %) in comparison with twigs (32 %), leaves and bark (20 % for both) (Fig. 3B). Only the treatments with twigs and roots, resulted in significant increases in total C content within the POM fraction (Fig. 3A).

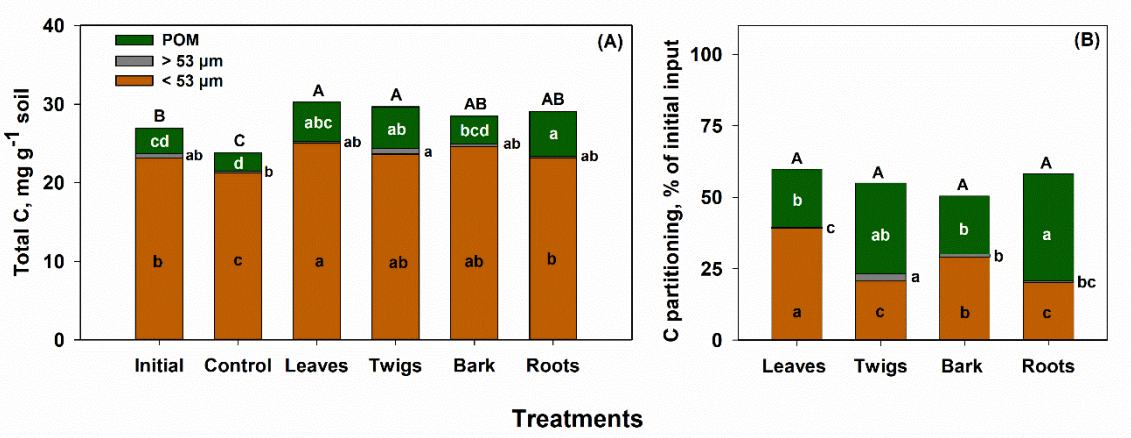

Fig. 3. Carbon distribution among soil organic matter fractions. A) Total carbon in soil organic matter fractions in pre-incubation (initial) and incubated samples for 200 days without plant litter (control) or following the application of leaves, twigs, bark and roots of eucalypt plants; B) Partitioning of litter derived-C among soil organic matter fractions: particulate organic matter (POM) with density < 1.8 g cm^{-3}, soil particle-size fraction greater than 53 µm (sand sized organic matter) and smaller than 53 µm, that is, mineral associated organic matter (MAOM). Uppercase letters compare total carbon content or total litter derived-C in soil organic matter fractions and lowercase letters compare the treatments within the same soil organic matter fraction. Means followed by the same letter do not differ among treatments at $p<0.05$ (Tukey's test).

3.4.4. Partitioning of native and litter-derived C in soil organic matter fractions

After the incubation, we observed significant reductions in “native” SOC content in the bulk soils as well as in the SOM fractions. The incubation resulted in reductions in total C content of “native” SOM in bulk soil (11.7 %) and MAOM (7.7%), with no significant differences observed among the treatments (Fig. 4B). In comparison, the total C content within the POM fraction was relatively more affected by the amendments with different litter types. Accordingly, incubation with twigs, bark and roots resulted in significant reductions of “native” POM-C as compared to the initial soil. All treatments resulted in reduction of “native” C in the sand-sized fraction, except for the soil samples incubated with twigs (Fig. 4D). In general, the losses of C in soil and SOM fractions were at least compensated by the addition of plant forest litter.

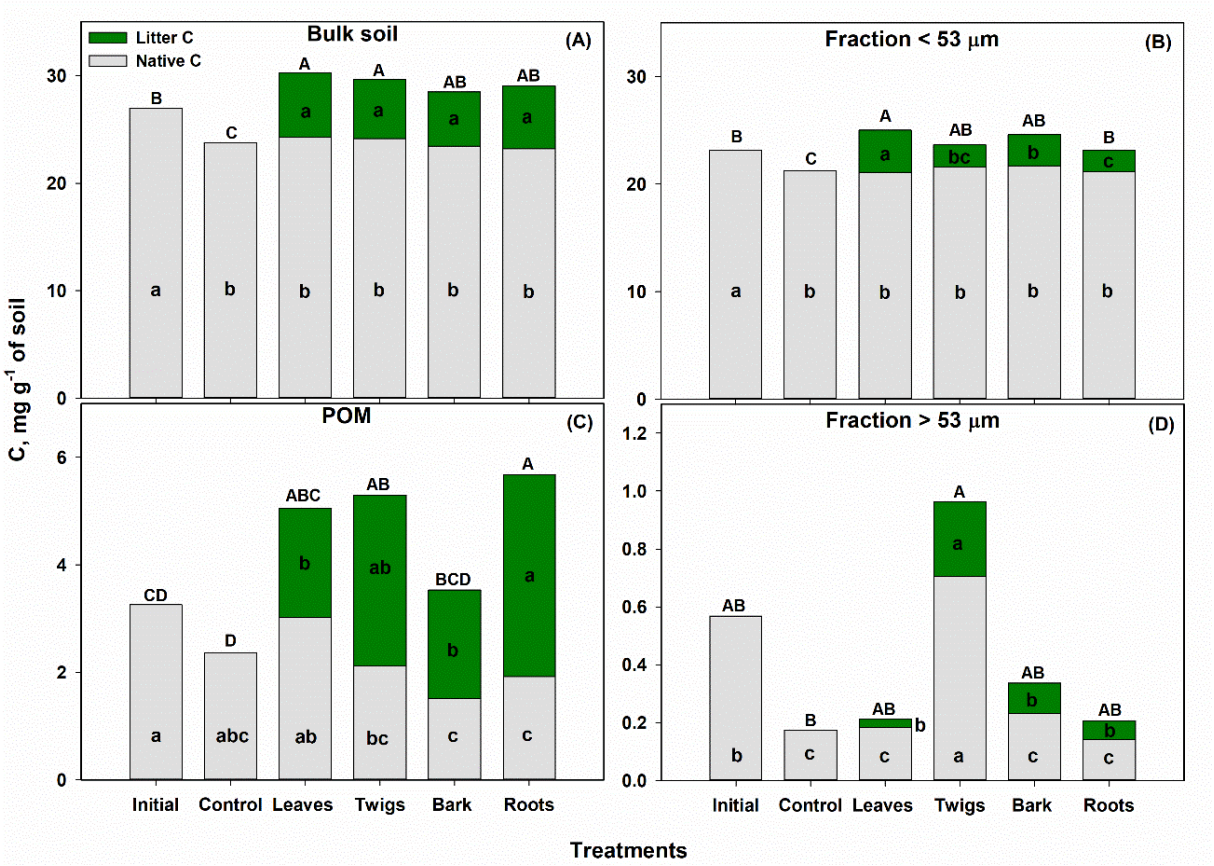

Fig. 4. Native and plant derived carbon contributions to soil and organic matter fractions in pre-incubation (initial) and incubated samples for 200 days without plant litter (control) or following the application of leaves, twigs, bark and roots of eucalypt plants: A) Bulk soil; B) fraction smaller than 53 µm (mineral associated organic matter); C) particulate organic matter (POM) with density < 1.8 g cm^{-3}; D) fraction greater than 53 µm (sand sized organic matter). Uppercase letters compare total carbon content in bulk soil or soil organic matter fractions and lowercase letters compare the C content

from a specific C pool (native or litter derived) among the treatments. Means followed by the same letter do not differ among treatments at $p<0.05$ (Tukey's test).

3.4.5. Chemical composition of SOM

The chemical composition of SOM fractions was determined using MMM based on ^{13}C-NMR CPMAS spectroscopy data to express the chemical composition in the relative amount of carbohydrates, proteins, lipids, lignin and carbonyl. As expected, carbohydrates were the predominant compound in both SOM fractions, representing 40 % of POM and 33 % of MAOM (averaged across all treatments). Yet, it worth noting that relative to the POM, the MAOM fraction was comparatively depleted in carbohydrates and lignin but enriched in proteins and carbonyl groups. These differences were not affected by the incubation as they also were evident in the control treatments (Fig. 5).

However, the incubation led to clear differences in the chemical composition of the POM fraction between the controls and the samples receiving plant litter. Consequently, a given plant litter tended to transfer its chemical characteristics into the POM. Among the most evident examples, soil samples amended with leaves, which is enriched in lipids and depleted in carbohydrates (Fig. 1C), showed POM with high lipid and relatively smaller proportion of carbohydrates (Fig. 5A). Conversely, the incubation with twigs resulted in POM with higher contents of carbohydrates and relatively lower amounts of lipids. Interestingly, the contribution of proteins in POM was about 10-12 %, and this proportion was almost constant among the different treatments but tended to be slightly higher in the samples receiving twigs. Yet, our data suggests that the protein content within the plant organs was about 10 % in the leaves and approximately 5 % in the other plant organs evaluated (Fig. 1). Therefore, it is puzzling that the POM could maintain an almost constant protein content considering the limited N content within the forest litter used, except for the leaves (Fig. 1). Moreover, this was not expected considering the significant entry of litter-C into the POM (Fig. 3 and 4).

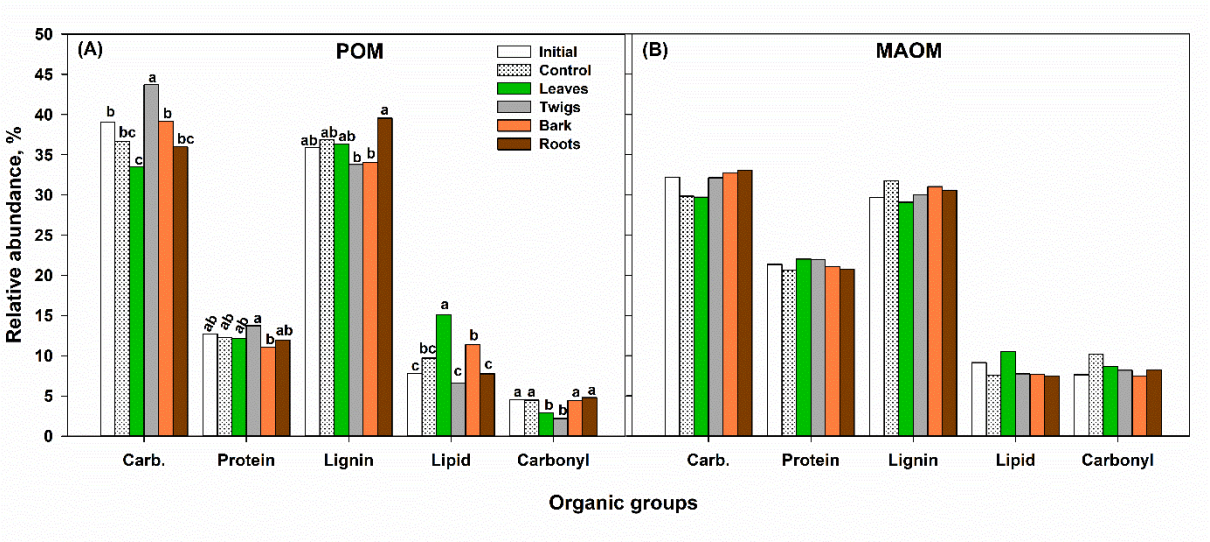

Fig. 5. Chemical composition of soil organic matter fractions based on NMR spectroscopy and relative abundance of the main organic groups (Carb. = carbohydrates, protein, lignin, lipid, carbonyl and char) as inferred from the Molecular Mixing Model; A) particulate organic matter and B) mineral associated organic matter. For a given organic group in particulate organic matter, means followed by the same lowercase letter do not differ among plant organs at $p<0.05$ (Tukey's test).

3.4.6. Microbial biomarkers and necromass contribution to SOC

Apparently, the incubation with forest litter led to a consistent decrease in total amino sugar contents relative to the control treatments (before or after the incubation) in bulk soil (Fig. 6A). Within the treatments receiving plant material, twigs resulted in the highest contents of amino sugars (77.3 mg g^{-1} SOC), while the lowest values were found in soil incubated with bark (45.8 mg g^{-1} SOC). Intermediate amounts of amino sugars were observed for the treatments with leaves and roots (63.1 and 68.3 mg g^{-1} SOC, respectively) (Fig. 6A).

We used the amounts of microbial biomarkers to estimate the contribution of microbial necromass to SOM. Because the microbial biomass was estimated based on the soil amino sugar contents, the trend observed in their results was comparable. The microbial necromass contribution to SOM appeared to decrease for the treatments amended with plant material relative to the initial soil and the control samples incubated for 200 days. The initial soil had approximately 73.8% of the SOM composed of microbial necromass, which increased up to 86.6 % for the incubation without plant residues (Fig. 6B). Within the treatments amended with plant materials, the microbial

necromass contribution to SOM were comparatively lower as follows: bark (38.1 %) < leaves (47.7 %) < roots (53.1 %) < twigs (59.1 %). Soil microbial-derived C was predominantly derived from fungi (70 %, average among treatments), while a smaller portion (30 %) was of bacterial origin. Only small variations were detected for bacterial derived-C in the samples, with significantly higher amounts being observed only for the initial soil. In contrast, more evident differences between the treatments were detected when considering fungal necromass, which followed the same trend of total contribution of microbial necromass to SOM (Fig. 6B).

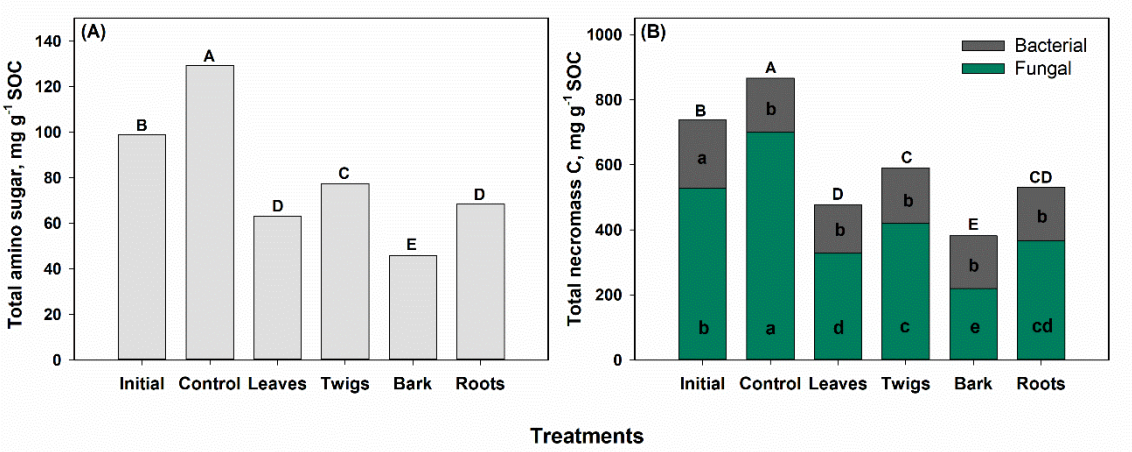

Fig. 6. Contribution of microbial-derived materials for bulk soil organic matter; (A) Total amino sugar contents and (B) the estimated bacterial and fungal necromass in pre-incubation (initial) and after the 200-days incubation of unamended soil (control) and amended soil samples with leaves, twigs, bark and roots of eucalypt plants. Uppercase letters compare total amino sugar contents or total necromass C, and lowercase letters compare necromass C from fungi or bacteria among the treatments. Means followed by the same letter do not differ among treatments at $p<0.05$ (Tukey's test).

3.5. Discussion

3.5.1. Forest litter decomposition and soil organic matter formation

Our results indicate that the decay of forest litter and the formation of POM and MAOM fractions can be put into a framework driven by *in vivo* and *ex vivo* pathways, and/or a combination of both. According to Liang *et al*. (2017), *in vivo* pathways are characterized by a 'divergence' in the chemistry of the original litter and SOM. Otherwise, *ex vivo* pathways are characterized by a relative 'convergence' between the original chemistry of the plant litter and SOM. Although our data suggests that the

formation of MAOM is dominated by *in vivo* pathways, the formation of POM appears to depend on a combination of both *ex vivo* and *in vivo* pathways.

Generally, our data is consistent with previous studies showing a strong influence of litter chemistry on its fate in soils. Accordingly, the decomposition of the forest litter appeared to be particularly dependent on the initial proportion of extractables (i.e. HWE and TSE) and structural components (i.e. CF and AUR). As such, aboveground litter materials (leaves, twigs and bark) which have high amounts of HWE (Fig. 1B), were respired at high rates (Fig. 2). This is consistent with previous observations that soil microorganisms can present high activity when using extractable compounds of plant litter (SHAHBAZ et al., 2017). Therefore, the interaction between decomposers and the chemistry of forest litter is critical for the formation of SOM pools. As such, plant components richer in nutrients and extractable compounds such as leaves may be preferentially transferred into MAOM via microbial growth (Fig. 3B). This pattern is consistent with the predominance of *in vivo* pathways (Liang *et al.*, 2017). Accordingly, previous studies have shown high microbial incorporation of soluble constituents of plant litter into the MAOM fraction (Lavallee *et al.,* 2018). The extractable compounds present in plant litter are known to be rapidly released after incorporation in the soil and subsequently favoring its incorporation by soil microorganisms (Cotrufo *et al.*, 2013; Shi *et al.*, 2013). Such dynamics were probably more relevant in the soils amended with aboveground litter, especially the leaves (Fig. 3B). Beyond the concentration of “labile” constituents, the nutrient content in plant tissues also can be important for SOM formation. As such, the bark tissue that is particularly enriched in Ca (Supplementary table 2) was fostering more the formation of MAOM compared to twigs (Fig. 3B). Hence, plant materials with higher nutrient contents are processed more efficiently by soil microorganisms resulting in higher MAOM formation (COTRUFO et al., 2013; LAVALLEE et al., 2018). Owing to the role of microorganisms incorporating the constituents of the plant litter, there is a significant difference (i.e. divergence) between the chemistry of the original substrate (Fig. 1) and SOM (Liang *et al.*, 2017). As such, the MAOM fraction had a protein content up to 20 % (Fig. 5), whereas even the leaf litter had only about 10 % of protein (Fig. 1).

As the concentration of structural components increases and nutrient contents decrease in plant tissues (e.g., roots), such materials tend to be less easily incorporated and/or transformed by soil microorganisms (BIRD; TORN, 2006;

BURDON, 2001; HICKS PRIES et al., 2017; VON LÜTZOW et al., 2006). To some extent, this trend is consistent with the concentration of AUR within the roots tissue we used (Fig. 1), and it is likely that this fraction was enriched in lignin, phenols and tannins (RASSE; RUMPEL; DIGNAC, 2005). This means that *ex vivo* pathways were comparatively more relevant in the soils that were amended with root litter, but certainly played a relevant role in the buildup of POM for all forest litter types (Fig. 3). However, only lignin appeared to occur at 30-40 % in all forest C litter and POM (Fig. 1 and Fig. 5), implying limited 'convergence' in these C pools. Accordingly, there was a significant 'divergence' between the chemistry of the substrates added and the composition of POM. As such, the concentration of carbohydrates varied between 40-70 % in plant litter (Fig. 1) but was reduced to 35-40 % in POM (Fig. 5). Furthermore, we observed a significant reduction in microbial amino sugars in bulk soil following the addition of all forest litter types (Fig. 6). Possibly, part of the microbial amino sugars was "immobilized" into the POM, which protein content remained constant in all treatments, despite the significant entry of litter-C into this fraction (Fig. 5). Hence, given the low content of protein within the plant tissues (Fig. 1), a 'convergence' would cause a proportional reduction in N-rich materials within the POM fraction in the treatments with litter addition relative to the controls. Therefore, it is reasonable that not only *ex vivo* pathways drive the formation of POM, and *in vivo* pathways are likely to be relevant as well. This trend also would be consistent with a simultaneous formation of both MAOM and POM (COTRUFO et al., 2015; FULTON-SMITH; COTRUFO, 2019; HADDIX; PAUL; COTRUFO, 2016).

3.5.2. Mineralization of "native" SOC as affected by litter biochemical composition

The mineralization of the "native" SOM is often (unintentionally) neglected in many studies linking litter chemistry and the buildup of soil organic C pools. Under the paradigm that microbial (by)products can contribute for both the buildup and decay of soil C pools, the mineralization of "native" SOM was probably linked to the mechanisms controlling the entry of plant litter into SOM fractions, especially through the *in vivo* pathways. Generally, the mineralization of "native" SOM was smaller in soils in the presence of leaf as compared to root, twigs and bark litter (Fig. 2). One possible

explanation is that the leaf litter provided an easier energy supply via bioavailable and easily degradable substrates (e.g., within its HWE fraction) together with balanced amounts of nutrients (e.g., C:N ratio) as compared to the other plant organs (CHEN et al., 2014). Consequently, the microorganisms assimilated and respired the leaf litter at high rates, and depended less on the supply of nutrients and/or metabolites associated with the “native” SOM (XIAO et al., 2015). Further, had the leaves, twigs and bark materials decomposing together as aboveground litter, the transfer of nutrients between them could have been facilitated (VERSINI et al., 2016).

Generally, roots are considered the major C source driving SOM buildup (ANGST et al., 2018, 2019; JACKSON et al., 2017; RASSE; RUMPEL; DIGNAC, 2005), but this was the litter type that caused the largest mineralization of “native” SOM in our study (Fig. 2). Similarly, samples treated with bark and twigs also caused more mineralization of “native” SOM compared to the effect observed in samples amended with leaf litter (Fig. 2). Thus, relative to the leaf litter, it is possible that the substrates found in roots, bark and twigs may provide imbalanced inputs of energy and/or nutrients. Hence, this could force the microorganisms to “mine” nutrients or substrates from the “native” SOM (CHEN et al., 2014). Another possibility is that the extracellular enzymes necessary for the depolymerization of lignocellulosic compounds abundant in twigs, bark and roots ended up inadvertently degrading part of the “native” SOM (COTRUFO et al., 2013; KUZYAKOV; FRIEDEL; STAHR, 2000; SHAHBAZ et al., 2017). For roots specifically, the accumulation of structural compounds (e.g., suberin) is thought to be one of the driving mechanisms responsible for its higher contribution to SOM as compared to aboveground inputs (JACKSON et al., 2017; RASSE; RUMPEL; DIGNAC, 2005). Overall, our results support the view that roots in forest ecosystems contribute more to SOM because it is already mixed into the soil and as such, in closer contact with the mineral matrix as compared to aboveground litter (LAVALLEE et al., 2018). However, oud data showed that litter chemistry still determines the magnitude of the mineralization of “native” SOM and the net C balance therein.

3.5.3. SOM formation, stabilization and accrual: the paradigm of aboveground vs. belowground litter inputs

Another important caveat in establishing a connection between litter chemistry and the pathways leading to SOM formation is related to the spatial constraints controlling C inputs to forest soils. In order to constrain this issue, we used our data to propose a conceptual framework that takes into account the vertical separation of above and belowground inputs to soil. Accordingly, aboveground litter inputs are more likely to be converted into more persistent SOM through microbial transformation via *in vivo* pathways as proposed by Liang *et al.* (2017). This is in line with the high respiration rates of aboveground litter (Fig. 2) coupled to its high contribution to MAOM (Fig. 3). However, these pathways are more effective close to the soil surface where all aboveground litter is deposited, but are ultimately hampered by a relatively limited contact between microbial (by)products and the soil mineral matrix. By averaging out the total contribution of leaves, twigs and bark to SOM fractions, the net C gain observed was 1.36 and 1.29 mg C g^{-1} soil for POM and for MAOM, respectively (Fig. 7). With respect to forest litter under field conditions, it can be expected that the aboveground litter should decompose into a mixture of various components, allowing the microorganisms to obtain C and nutrients from various plant derived materials (VERSINI et al., 2016). For instance, leaves and bark that are more enriched in nutrients (supplementary table 2) could be beneficial for the microbial decomposition of twigs and incorporation of its constituents into SOM.

In sharp contrast with aboveground litter, the contribution of roots to SOM depends proportionally more on *ex vivo* pathways, since it is usually less assimilated by microorganisms (Fig. 2). As a result, root litter contributes proportionally more to POM, which net C gain was about 2.42 mg C g^{-1} soil (Fig. 7). This value was almost 78 % higher than the average accumulation of C within the POM fraction after the application of aboveground litter (Fig. 7). However, root tissues can also contribute to MAOM, but the net C gain was only 0.02 mg C g^{-1} soil (Fig. 7). Hence, the incorporation of roots into MAOM through *in vivo* pathways comes with a 'penalty' owing to the extra mineralization of "native" MAOM. Although root litter and the soil mineral matrix are in close contact which should favor SOM build up, the process is ultimately hampered by litter chemistry. Nonetheless, nutrients and soluble compounds released from

aboveground litter materials could facilitate the microbial transformation of root-derived C into SOM. However, several studies have indicated limited effects of aboveground litter on SOM at depths below 5 cm, even under field conditions where bioturbation is not restricted (ANGST et al., 2019; COTRUFO et al., 2015; LIEBMANN et al., 2020). Ideally, SOM accrual would require both pathways to be simultaneously active, which is most likely to take place within the first few centimeters of the topsoil (Fig. 7). Overall, when the constraints due to the vertical separation of above and belowground C inputs to soils are considered, the influence of litter chemistry on the pathways controlling SOM formation becomes more tangible. These aspects are critical to model and predict soil C dynamics in forest ecosystems in response to environmental changes brought about by increasing atmospheric levels of CO_2.

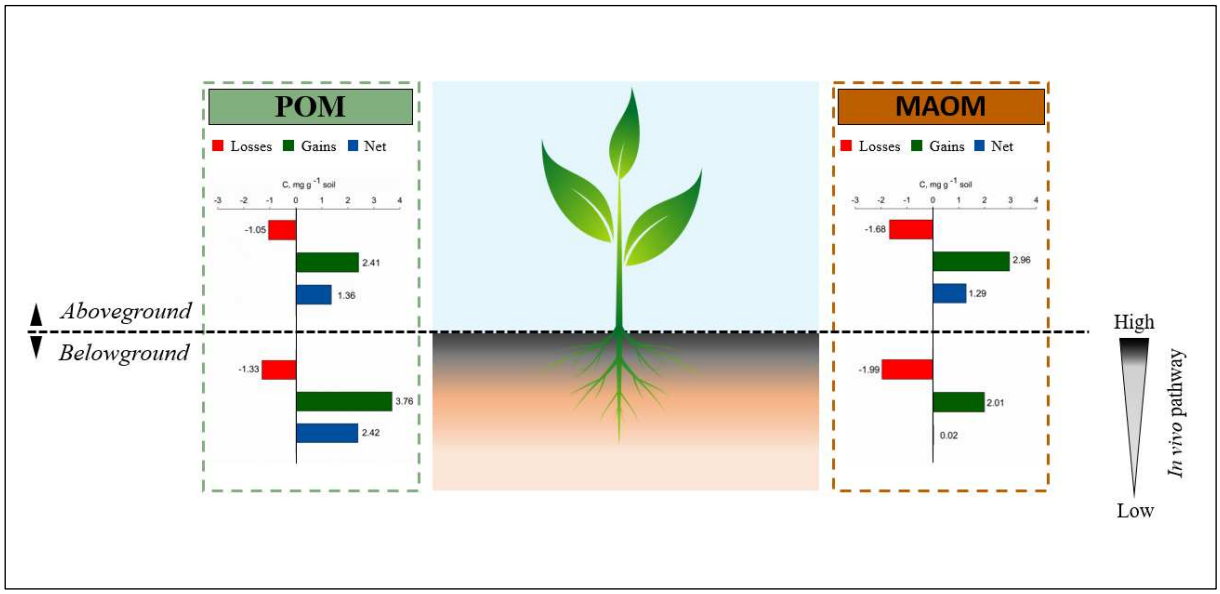

Figure 7. Conceptual representation of the effects of plant litter chemistry and input location (above and belowground) on SOM formation and the mineralization of "native" SOM. The efficiency of the *in vivo* pathways is high close to the soil surface where a mixture of litter types is added aboveground with reduced the mineralization of "native" SOM. Belowground, the efficiency of *in vivo* pathways controlling SOM formation decreases owing to limitations imposed by the chemistry of root tissues and high mineralization of "native" SOM. POM = particulate organic matter with density <1.8 g cm^{-3}; MAOM = mineral associated organic matter. Red bars represent averaged C losses (C-CO_2 respired from "native" SOM along the incubation period), green bars represent total C gains (litter-derived C transferred to POM and MAOM fractions), and blue bars represents the net C balance, i.e. the difference between C losses and C gains for the POM and MAOM.

3.6. Conclusions

In this study, we demonstrate that the influence of litter chemistry on the pathways through which forest litter is converted into SOM cannot be overlooked. Generally, SOM formation through *in vivo* pathways that are controlled by the microbial incorporation of plant substrates is particularly efficient for leaf litter. As such, leaf litter appears to provide a balanced supply of nutrients and substrates that can be easily metabolized. Given that leaf litter was respired at high rates, its contribution to MAOM indicates a significant role of *in vivo* pathways. As a result, the decomposition of such materials results in less degradation of “native” SOM due to positive “priming effect”. On the other extreme, roots are more enriched in hydrophobic and structural substrates that are more difficult to be assimilated by microorganisms. Hence, *ex vivo* pathways are proportionally more important for SOM formation from roots as compared to aboveground litter. Moreover, roots contribute more to POM than to MAOM, and also caused higher mineralization of “native” SOM than leaves. Nonetheless, our results suggest that *in vivo* pathways can be as important as *ex vivo* routes in the formation of POM for all forest litter, but especially for roots. Therefore, the connection between litter chemistry and the pathways controlling SOM formation should be included in model frameworks. However, the predictive power of such frameworks should not be satisfactory without replicating the decomposition of “native” SOM and considering the vertical separation of litter inputs above and belowground in forest soils.

3.7. References

ALMEIDA, L. F. J. et al. Soil organic matter formation as affected by eucalypt litter biochemistry — Evidence from an incubation study. **Geoderma**, v. 312, n. March 2017, p. 121–129, fev. 2018.

ANGST, G. et al. Soil organic carbon stocks in topsoil and subsoil controlled by parent material, carbon input in the rhizosphere, and microbial-derived compounds. **Soil Biology and Biochemistry**, v. 122, n. July, p. 19–30, 2018.

ANGST, G. et al. Soil organic carbon stability in forests: Distinct effects of tree species identity and traits. **Global Change Biology**, v. 25, n. 4, p. 1529–1546, 2019.

BIRD, J. A.; TORN, M. S. Fine Roots vs. Needles: A Comparison of 13C and 15N Dynamics in a Ponderosa Pine Forest Soil. **Biogeochemistry**, v. 79, n. 3, p. 361–382, jul. 2006.

BURDON, J. Are the traditional concepts the structures of humic substances realistic? **Soil Science**, v. 166, n. 11, p. 752–769, 2001.

CHEN, R. et al. Soil C and N availability determine the priming effect: Microbial N mining and stoichiometric decomposition theories. **Global Change Biology**, v. 20, n. 7, p. 2356–2367, 2014.

CLARK, R. B. Characterization of phosphatase of intact maize roots. **Journal of agricultural and food chemistry**, v. 23, n. 3, p. 458–460, 1975.

COTRUFO, M. F. et al. The Microbial Efficiency-Matrix Stabilization (MEMS) framework integrates plant litter decomposition with soil organic matter stabilization: Do labile plant inputs form stable soil organic matter? **Global Change Biology**, v. 19, n. 4, p. 988–995, 2013.

COTRUFO, M. F. et al. Formation of soil organic matter via biochemical and physical pathways of litter mass loss. **Nature Geoscience**, v. 8, n. 10, p. 776–779, 2015.

CRAINE, J. M.; MORROW, C.; FIERER, N. Microbial nitrogen limitation increases decomposition. **Ecology**, v. 88, n. 8, p. 2105–2113, 2007.

DENEF, K.; GALDO, I. Assessment of soil C and N stocks and fractions across 11 European soils under varying land uses. **Open Journal of Soil Science**, v. 3, n. November, p. 297–313, 2013.

FONTAINE, S.; MARIOTTI, A.; ABBADIE, L. The priming effect of organic matter: A question of microbial competition? **Soil Biology and Biochemistry**, v. 35, n. 6, p. 837–843, 2003.

FULTON-SMITH, S.; COTRUFO, M. F. Pathways of soil organic matter formation from above and belowground inputs in a Sorghum bicolor bioenergy crop. **GCB Bioenergy**, v. 11, n. 8, p. 971–987, 2019.

HADDIX, M. L.; PAUL, E. A.; COTRUFO, M. F. Dual, differential isotope labeling shows the preferential movement of labile plant constituents into mineral-bonded soil organic matter. **Global Change Biology**, v. 22, n. 6, p. 2301–2312, 2016.

HICKS PRIES, C. E. et al. Long term decomposition: the influence of litter type and soil horizon on retention of plant carbon and nitrogen in soils. **Biogeochemistry**, v. 134, n. 1–2, p. 5–16, 2017.

JACKSON, R. B. et al. The Ecology of Soil Carbon: Pools, Vulnerabilities, and Biotic and Abiotic Controls. **Annual Review of Ecology, Evolution, and Systematics**, v. 48, n. 1, p. 419–445, 2017.

KOPITTKE, P. M. et al. Nitrogen-rich microbial products provide new organo-mineral associations for the stabilization of soil organic matter. **Global Change Biology**, v. 24, n. 4, p. 1762–1770, abr. 2018.

KOPITTKE, P. M. et al. Soil organic matter is stabilized by organo-mineral associations through two key processes: The role of the carbon to nitrogen ratio. **Geoderma**, v. 357, n. June 2019, p. 113974, 2020.

KUZYAKOV, Y.; FRIEDEL, J. K.; STAHR, K. Review of mechanisms and quantification of priming effects. **Soil Biology and Biochemistry**, v. 32, n. 11–12, p. 1485–1498, 2000.

LAVALLEE, J. M. et al. Incorporation of shoot versus root-derived 13 C and 15 N into mineral-associated organic matter fractions: results of a soil slurry incubation with dual-labelled plant material. **Biogeochemistry**, v. 137, n. 3, p. 379–393, 2018.

LEHMANN, J.; KLEBER, M. The contentious nature of soil organic matter. **Nature**, v. 528, n. 7580, p. 60–68, 2015.

LIANG, C. et al. Quantitative assessment of microbial necromass contribution to soil organic matter. **Global Change Biology**, n. September, 2019.

LIANG, C.; SCHIMEL, J. P.; JASTROW, J. D. The importance of anabolism in microbial control over soil carbon storage. **Nature Microbiology**, v. 2, n. 8, 2017.

LIEBMANN, P. et al. Relevance of aboveground litter for soil organic matter formation – a soil profile perspective. **Biogeosciences Discussions**, n. January, p. 1–29, 2020.

LIM, CHIN HUAT & JACKSON, M. Dissolution for Total Elemental Analysis. In: **METHODS OF SOIL ANALYSIS Part 2, Second Edition**. [s.l: s.n.]. p. 1–12.

LYU, M. et al. Litter quality and site characteristics interact to affect the response of priming effect to temperature in subtropical forests. **Functional Ecology**, v. 33, n. 11, p. 2226–2238, 2019.

MELILLO, J. M. et al. Nitrogen and Lignin Control of Hardwood Leaf Litter Decomposition Dynamics. v. 63, n. 3, p. 621–626, 1982.

MILCU, A. et al. Identification of General Patterns of Nutrient and Labile Carbon Control on Soil Carbon Dynamics Across a Successional Gradient. **Ecosystems**, v. 14, n. 5, p. 710–719, 2011.

MWAFULIRWA, L. et al. Ryegrass root and shoot residues differentially affect short-term priming of soil organic matter and net soil C-balance. **European Journal of Soil Biology**, v. 93, n. January, p. 103096, 2019.

NELSON, P. N.; BALDOCK, J. A. Estimating the molecular composition of a diverse range of natural organic materials from solid-state 13 C NMR and elemental analyses. **Biogeochemistry**, v. 72, n. 1, p. 1–34, 2005.

NORTH, P. F. Towards an absolute measurement of soil structural stability using ultrasound. **Journal of Soil Science**, v. 27, n. 4, p. 451–459, 1976.

RASSE, D. P.; RUMPEL, C.; DIGNAC, M.-F. Is soil carbon mostly root carbon? Mechanisms for a specific stabilisation. **Plant and Soil**, v. 269, n. 1–2, p. 341–356,

fev. 2005.

SHAHBAZ, M. et al. Microbial decomposition of soil organic matter is mediated by quality and quantity of crop residues: mechanisms and thresholds. **Biology and Fertility of Soils**, v. 53, n. 3, p. 287–301, 2017.

SHI, A.; PENFOLD, C.; MARSCHNER, P. Decomposition of roots and shoots of perennial grasses and annual barley-separately or in two residue mixes. **Biology and Fertility of Soils**, v. 49, n. 6, p. 673–680, 2013.

STEWART, C. E. et al. Soil carbon saturation: Implications for measurable carbon pool dynamics in long-term incubations. **Soil Biology and Biochemistry**, v. 41, n. 2, p. 357–366, 2009.

VERSINI, A. et al. Nitrogen dynamics within and between decomposing leaves, bark and branches in Eucalyptus planted forests. **Soil Biology and Biochemistry**, v. 101, p. 55–64, 2016.

VON LÜTZOW, M. et al. Stabilization of organic matter in temperate soils: mechanisms and their relevance under different soil conditions - a review. **European Journal of Soil Science**, v. 57, n. 4, p. 426–445, ago. 2006.

XIAO, C. et al. Priming of soil organic matter decomposition scales linearly with microbial biomass response to litter input in steppe vegetation. **Oikos**, v. 124, n. 5, p. 649–657, 2015.

3.7. Supplementary information

Supplementary table 1. Total carbon content and isotopic composition of leaves, twigs, bark and roots of eucalyptus enriched with ^{13}C used for the incubation experiment.

Plant organ	C, %	Delta PDB, ‰
Leaves	44.09 ± 0.39	425.11 ± 10.93
Twigs	42.90 ± 1.04	359.64 ± 31.95
Bark	41.64 ± 0.17	319.06 ± 16.66
Roots	43.56 ± 1.62	377.95 ± 35.14

Supplementary table 2. Contents of macronutrients in the plant material used for the incubation experiment.

Plant organ	N	K	Ca	Mg	S	P
	..... g kg^{-1}					..... mg kg^{-1} ...
Leaves	17.24 ± 0.21	20.78 ± 1.84	13.74 ± 0.07	3.02 ± 0.13	2.13 ± 0.13	2.17 ± 0.07
Twigs	7.74 ± 0.12	16.27 ± 1.21	13.68 ± 0.16	1.35 ± 0.02	0.87 ± 0.01	2.66 ± 0.12
Bark	5.74 ± 0.06	16.41 ± 0.39	32.32 ± 1.62	1.97 ± 0.09	1.28 ± 0.13	3.20 ± 0.22
Roots	8.55 ± 0.32	11.36 ± 0.57	6.71 ± 0.22	1.64 ± 0.07	1.62 ± 0.12	1.62 ± 0.04

N – Nitrogen, K – Potassium, Ca – Calcium, Mg – Magnesium, S – Sulfur, P – Phosphorus

Supplementary table 3. Total elemental contents in pre-incubation (initial) and incubated samples without plant litter (control) or following the application of leaves, twigs, bark and roots of eucalypt plants.

Treatments	Elements								
	Al	Ca	Fe	K	Mg	Mn	Na	P	S
	..... mg g^{-1}								
Initial	52.72 ab	0.64 c	30.01 a	0.47 e	0.36 a	0.20 a	17.74 c	0.35 a	0.34 ab
Control	48.69 b	0.62 c	31.03 a	0.87 d	0.38 a	0.17 a	15.24 cd	0.37 a	0.30 ab
Leaves	49.57 ab	0.91 b	28.58 a	2.21 a	0.51 a	0.21 a	20.65 b	0.37 a	0.34 ab
Twigs	55.51 a	1.10 ab	30.60 a	2.04 b	0.43 a	0.20 a	32.84 a	0.41 a	0.36 a
Bark	47.66 b	1.19 a	27.08 a	1.54 c	0.35 a	0.18 a	14.05 d	0.36 a	0.29 b
Roots	51.94 ab	0.63 c	29.28 a	0.44 e	0.38 a	0.20 a	15.65 cd	0.33 a	0.31 ab

'

4. GENERAL CONCLUSIONS

The present study contributed to significant advances on the understanding of litter chemical composition effects on soil organic matter dynamics. The complementarity between molecular diversity of the biochemical fractions of eucalypt plant tissues obtained from NMR-MMM and thermochemolysis-GC-MS experiments highlights the efficiency of combined methods in SOM studies. Additionally, we could also demonstrate that the substrate selection and thermodynamic constraints on microbial metabolism are more relevant for the respiration of biochemical fractions of eucalypt plant tissues than their inherent molecular diversity. Moreover, the incubation of plant organs with distinct composition allowed us to link litter chemistry with the SOM formation pathways and also its effect on “native” SOM. As such, plant materials considered labile are preferentially incorporated in MAOM through *in vivo* pathway and causes less priming. Conversely, fractions considered recalcitrant contribute more to POM through *ex vivo* pathway and leads to relatively higher priming. Moreover, we used the data obtained in our study to propose a framework of SOM formation in forest ecosystems, in which litter fractions with distinct composition are spatially constrained. Hence, we predict that under forest ecosystems, SOM formation via *in vivo* pathways might also be spatially constrained and more pronounced in the zone of influence of aboveground litter inputs.

5. GENERAL REFERENCES

ALMEIDA, L. F. J. et al. Soil organic matter formation as affected by eucalypt litter biochemistry — Evidence from an incubation study. **Geoderma**, v. 312, n. March 2017, p. 121–129, fev. 2018.

ANGST, G. et al. Soil organic carbon stocks in topsoil and subsoil controlled by parent material, carbon input in the rhizosphere, and microbial-derived compounds. **Soil Biology and Biochemistry**, v. 122, n. July, p. 19–30, 2018.

ANGST, G. et al. Soil organic carbon stability in forests: Distinct effects of tree species identity and traits. **Global Change Biology**, v. 25, n. 4, p. 1529–1546, 2019.

BERG, B. et al. Relationships between nitrogen, acid-unhydrolyzable residue, and climate among tree foliar litters. **Canadian Journal of Forest Research**, v. 43, n. 1, p. 103–107, 2013.

BIRD, J. A.; TORN, M. S. Fine Roots vs. Needles: A Comparison of 13C and 15N Dynamics in a Ponderosa Pine Forest Soil. **Biogeochemistry**, v. 79, n. 3, p. 361–382, jul. 2006.

BRADFORD, M. A. et al. Empirical evidence that soil carbon formation from plant inputs is positively related to microbial growth. **Biogeochemistry**, v. 113, n. 1–3, p. 271–281, 2013.

BRADLEY, R. Dynamics of nitrogen associated to acid insoluble substances derived from plant litter. **Communications in Soil Science and Plant Analysis**, v. 33, n. 7–8, p. 1277–1290, 2002.

BURDON, J. Are the traditional concepts the structures of humic substances realistic? **Soil Science**, v. 166, n. 11, p. 752–769, 2001.

CHAPUIS-LARDY, L.; CONTOUR-ANSEL, D.; BERNHARD-REVERSAT, F. High-performance liquid chromatography of water-soluble phenolics in leaf litter of three Eucalyptus hybrids (Congo). **Plant Science**, v. 163, n. 2, p. 217–222, 2002.

CHEN, R. et al. Soil C and N availability determine the priming effect: Microbial N mining and stoichiometric decomposition theories. **Global Change Biology**, v. 20, n. 7, p. 2356–2367, 2014.

CLARK, R. B. Characterization of phosphatase of intact maize roots. **Journal of agricultural and food chemistry**, v. 23, n. 3, p. 458–460, 1975.

COTRUFO, M. F. et al. The Microbial Efficiency-Matrix Stabilization (MEMS) framework integrates plant litter decomposition with soil organic matter stabilization: Do labile plant inputs form stable soil organic matter? **Global Change Biology**, v. 19, n. 4, p. 988–995, 2013.

COTRUFO, M. F. et al. Formation of soil organic matter via biochemical and physical pathways of litter mass loss. **Nature Geoscience**, v. 8, n. 10, p. 776–779, 2015.

CRAINE, J. M.; MORROW, C.; FIERER, N. Microbial nitrogen limitation increases decomposition. **Ecology**, v. 88, n. 8, p. 2105–2113, 2007.

DAVIDSON, E. A.; JANSSENS, I. A. Temperature sensitivity of soil carbon

decomposition and feedbacks to climate change. **Nature**, v. 440, n. 7081, p. 165–173, 2006.

DENEF, K.; GALDO, I. Assessment of soil C and N stocks and fractions across 11 European soils under varying land uses. **Open Journal of Soil Science**, v. 3, n. November, p. 297–313, 2013.

DUNGAIT, J. A J. et al. Soil organic matter turnover is governed by accessibility not recalcitrance. **Global Change Biology**, v. 18, n. 6, p. 1781–1796, jun. 2012.

FONTAINE, S.; MARIOTTI, A.; ABBADIE, L. The priming effect of organic matter: A question of microbial competition? **Soil Biology and Biochemistry**, v. 35, n. 6, p. 837–843, 2003.

FREI, M. Lignin: Characterization of a multifaceted crop component. **The Scientific World Journal**, v. 2013, p. 1–25, 2013.

FULTON-SMITH, S.; COTRUFO, M. F. Pathways of soil organic matter formation from above and belowground inputs in a Sorghum bicolor bioenergy crop. **GCB Bioenergy**, v. 11, n. 8, p. 971–987, 2019.

GRANDY, A. S.; NEFF, J. C. Molecular C dynamics downstream: The biochemical decomposition sequence and its impact on soil organic matter structure and function. **Science of the Total Environment**, v. 404, n. 2–3, p. 297–307, 2008.

HADDIX, M. L.; PAUL, E. A.; COTRUFO, M. F. Dual, differential isotope labeling shows the preferential movement of labile plant constituents into mineral-bonded soil organic matter. **Global Change Biology**, v. 22, n. 6, p. 2301–2312, 2016.

HATCHER, P. G. et al. Comparison of two thermochemolytic methods for the analysis of lignin in decomposing gymnosperm wood: the CuO oxidation method and the method of thermochemolysis with tetramethylammonium hydroxide (TMAH). **Organic Geochemistry**, v. 23, n. 10, p. 881–888, 1995.

HEDGES, J. I.; KEIL, R. G. Organic geochemical perspectives on estuarine processes: sorption reactions and consequences. **Marine Chemistry**, v. 65, n. 1–2, p. 55–65, maio 1999.

HICKS PRIES, C. E. et al. Long term decomposition: the influence of litter type and soil horizon on retention of plant carbon and nitrogen in soils. **Biogeochemistry**, v. 134, n. 1–2, p. 5–16, 2017.

HILLI, S. et al. What is the composition of AIR? Pyrolysis-GC-MS characterization of acid-insoluble residue from fresh litter and organic horizons under boreal forests in southern Finland. **Geoderma**, v. 179–180, p. 63–72, 2012.

HOFFMANN, B. et al. Abundance and distribution of leaf wax n-alkanes in leaves of Acacia and Eucalyptus trees along a strong humidity gradient in northern Australia. **Organic Geochemistry**, v. 62, p. 62–67, set. 2013.

HUANG, W. et al. Trade-offs in soil carbon protection mechanisms under aerobic and anaerobic conditions. **Global Change Biology**, v. 26, n. 6, p. 3726–3737, 2020.

IUSS WORKING GROUP WRB. **World reference base for soil resources 2014. International soil classification system for naming soils and creating legends for soil maps**. [s.l: s.n.].

JACKSON, R. B. et al. The Ecology of Soil Carbon: Pools, Vulnerabilities, and Biotic

and Abiotic Controls. **Annual Review of Ecology, Evolution, and Systematics**, v. 48, n. 1, p. 419–445, 2017.

JILLING, A. et al. Minerals in the rhizosphere: overlooked mediators of soil nitrogen availability to plants and microbes. **Biogeochemistry**, v. 139, n. 2, p. 103–122, 2018.

KALLENBACH, C. M.; FREY, S. D.; GRANDY, A. S. Direct evidence for microbial-derived soil organic matter formation and its ecophysiological controls. **Nature Communications**, v. 7, p. 1–10, 2016.

KEILUWEIT, M. et al. Are oxygen limitations under recognized regulators of organic carbon turnover in upland soils? **Biogeochemistry**, v. 127, n. 2–3, p. 157–171, 22 fev. 2016.

KLEBER, M. What is recalcitrant soil organic matter? **Environmental Chemistry**, v. 7, n. 4, p. 320–332, 2010.

KLEBER, M. et al. **Mineral-Organic Associations: Formation, Properties, and Relevance in Soil Environments**. [s.l.] Elsevier Ltd, 2015. v. 130

KLEBER, M.; SOLLINS, P.; SUTTON, R. A conceptual model of organo-mineral interactions in soils: self-assembly of organic molecular fragments into zonal structures on mineral surfaces. **Biogeochemistry**, v. 85, n. 1, p. 9–24, jun. 2007.

KLOTZBÜCHER, T. et al. A study of lignin degradation in leaf and needle litter using 13C-labelled tetramethylammonium hydroxide (TMAH) thermochemolysis: Comparison with CuO oxidation and van Soest methods. **Organic Geochemistry**, v. 42, n. 10, p. 1271–1278, nov. 2011.

KNIGHT, T. G.; WALLWORK, M. A. B.; SEDGLEY, M. Leaf epicuticular wax and cuticle ultrastructure of four Eucalyptus species and their hybrids. **International Journal of Plant Sciences**, v. 165, n. 1, p. 27–36, jan. 2004.

KÖGEL-KNABNER, I. The macromolecular organic composition of plant and microbial residues as inputs to soil organic matter. **Soil Biology and Biochemistry**, v. 34, n. 2, p. 139–162, fev. 2002.

KÖGEL-KNABNER, I.; RUMPEL, C. Advances in molecular approaches for understanding soil organic matter composition, origin, and turnover: A historical overview. In: **Advances in Agronomy**. 1. ed. [s.l.] Elsevier Inc., 2018. p. 1–48.

KOLATTUKUDY, P. E. Structure, biosynthesis, and biodegradation of cutin and suberin. **Annual Review of Plant Physiology**, v. 32, n. 1, p. 539–567, jun. 1981.

KOPITTKE, P. M. et al. Nitrogen-rich microbial products provide new organo-mineral interactions for the stabilization of soil organic matter. **Global Change Biology**, n. July, p. 1–9, 2017.

KOPITTKE, P. M. et al. Nitrogen-rich microbial products provide new organo-mineral associations for the stabilization of soil organic matter. **Global Change Biology**, v. 24, n. 4, p. 1762–1770, abr. 2018.

KOPITTKE, P. M. et al. Soil organic matter is stabilized by organo-mineral associations through two key processes: The role of the carbon to nitrogen ratio. **Geoderma**, v. 357, n. June 2019, p. 113974, 2020.

KUZYAKOV, Y.; FRIEDEL, J. K.; STAHR, K. Review of mechanisms and quantification of priming effects. **Soil Biology and Biochemistry**, v. 32, n. 11–12, p. 1485–1498,

2000.

LAJTHA, K. et al. The detrital input and removal treatment (DIRT) network: Insights into soil carbon stabilization. **Science of The Total Environment**, v. 640–641, n. June, p. 1112–1120, 2018.

LAL, R. Forest soils and carbon sequestration. **Forest Ecology and Management**, v. 220, n. 1–3, p. 242–258, 2005.

LAROWE, D. E.; VAN CAPPELLEN, P. Degradation of natural organic matter: A thermodynamic analysis. **Geochimica et Cosmochimica Acta**, v. 75, n. 8, p. 2030–2042, 2011.

LAVALLEE, J. M. et al. Incorporation of shoot versus root-derived 13 C and 15 N into mineral-associated organic matter fractions: results of a soil slurry incubation with dual-labelled plant material. **Biogeochemistry**, v. 137, n. 3, p. 379–393, 2018.

LEHMANN, J. et al. Persistence of soil organic carbon caused by functional complexity. **Nature Geoscience**, jul. 2020.

LEHMANN, J.; KLEBER, M. The contentious nature of soil organic matter. **Nature**, v. 528, n. 7580, p. 60–68, 2015.

LIANG, C. et al. Quantitative assessment of microbial necromass contribution to soil organic matter. **Global Change Biology**, n. September, 2019.

LIANG, C.; SCHIMEL, J. P.; JASTROW, J. D. The importance of anabolism in microbial control over soil carbon storage. **Nature Microbiology**, v. 2, n. 8, 2017.

LIEBMANN, P. et al. Relevance of aboveground litter for soil organic matter formation – a soil profile perspective. **Biogeosciences Discussions**, n. January, p. 1–29, 2020.

LIM, CHIN HUAT & JACKSON, M. Dissolution for Total Elemental Analysis. In: **METHODS OF SOIL ANALYSIS Part 2, Second Edition**. [s.l: s.n.]. p. 1–12.

LYU, M. et al. Litter quality and site characteristics interact to affect the response of priming effect to temperature in subtropical forests. **Functional Ecology**, v. 33, n. 11, p. 2226–2238, 2019.

MALIK, A. A. et al. Soil microbial communities with greater investment in resource acquisition have lower growth yield. **Soil Biology and Biochemistry**, v. 132, n. November 2018, p. 36–39, maio 2019.

MARSCHNER, B. et al. How relevant is recalcitrance for the stabilization of organic matter in soils? **Journal of Plant Nutrition and Soil Science**, v. 171, n. 1, p. 91–110, 2008.

MELILLO, J. M. et al. Nitrogen and Lignin Control of Hardwood Leaf Litter Decomposition Dynamics. v. 63, n. 3, p. 621–626, 1982.

MILCU, A. et al. Identification of General Patterns of Nutrient and Labile Carbon Control on Soil Carbon Dynamics Across a Successional Gradient. **Ecosystems**, v. 14, n. 5, p. 710–719, 2011.

MWAFULIRWA, L. et al. Ryegrass root and shoot residues differentially affect short-term priming of soil organic matter and net soil C-balance. **European Journal of Soil Biology**, v. 93, n. January, p. 103096, 2019.

NELSON, P. N.; BALDOCK, J. A. Estimating the molecular composition of a diverse

range of natural organic materials from solid-state 13 C NMR and elemental analyses. **Biogeochemistry**, v. 72, n. 1, p. 1–34, 2005.

NORTH, P. F. Towards an absolute measurement of soil structural stability using ultrasound. **Journal of Soil Science**, v. 27, n. 4, p. 451–459, 1976.

OSAWA, T.; NAMIKI, M. Natural antioxidants isolated from Eucalyptus leaf waxes. **Journal of Agricultural and Food Chemistry**, v. 33, n. 5, p. 777–780, set. 1985.

OSONO, T.; TAKEDA, H.; AZUMA, J. I. Carbon isotope dynamics during leaf litter decomposition with reference to lignin fractions. **Ecological Research**, v. 23, n. 1, p. 51–55, 2008.

PRESTON, C. M.; NAULT, J. R.; TROFYMOW, J. A. Chemical changes during 6 years of decomposition of 11 litters in some Canadian forest sites. Part 2. 13C abundance, solid-state 13C NMR spectroscopy and the meaning of “lignin”. **Ecosystems**, v. 12, n. 7, p. 1078–1102, 2009.

PRESTON, C. M.; TROFYMOW, J. A. Variability in litter quality and its relationship to litter decay in Canadian forests. **Canadian Journal of Botany**, v. 78, n. 10, p. 1269–1287, 2000.

PRESTON, C. M.; TROFYMOW, J. A. The chemistry of some foliar litters and their sequential proximate analysis fractions. **Biogeochemistry**, v. 126, n. 1–2, p. 197–209, 2015.

RAMIN, K. I.; ALLISON, S. D. Bacterial tradeoffs in growth rate and extracellular enzymes. **Frontiers in Microbiology**, v. 10, n. December, p. 1–10, dez. 2019.

RASSE, D. P.; RUMPEL, C.; DIGNAC, M.-F. Is soil carbon mostly root carbon? Mechanisms for a specific stabilisation. **Plant and Soil**, v. 269, n. 1–2, p. 341–356, fev. 2005.

RYAN, M. G.; MELILLO, J. M.; RICCA, A. A comparison of methods for determining proximate carbon fractions of forest litter. **Canadian journal of Forest Research**, n. 20, p. 166–171, 1990.

SANTOS, S. A. O. et al. Characterization of phenolic components in polar extracts of Eucalyptus globulus Labill. bark by high-performance liquid chromatography–mass spectrometry. **Journal of Agricultural and Food Chemistry**, v. 59, n. 17, p. 9386–9393, set. 2011.

SCHMIDT, M. W. I. et al. Persistence of soil organic matter as an ecosystem property. **Nature**, v. 478, n. 7367, p. 49–56, 5 out. 2011.

SHAHBAZ, M. et al. Microbial decomposition of soil organic matter is mediated by quality and quantity of crop residues: mechanisms and thresholds. **Biology and Fertility of Soils**, v. 53, n. 3, p. 287–301, 2017.

SHI, A.; PENFOLD, C.; MARSCHNER, P. Decomposition of roots and shoots of perennial grasses and annual barley-separately or in two residue mixes. **Biology and Fertility of Soils**, v. 49, n. 6, p. 673–680, 2013.

SJÖBERG, G. et al. Degradation of hemicellulose, cellulose and lignin in decomposing spruce needle litter in relation to N. **Soil Biology and Biochemistry**, v. 36, n. 11, p. 1761–1768, 2004.

SLUITER, J. B. et al. Compositional analysis of lignocellulosic feedstocks. 1. Review

and description of methods. **Journal of Agricultural and Food Chemistry**, v. 58, n. 16, p. 9043–9053, ago. 2010.

STEWART, C. E. et al. Soil carbon saturation: Implications for measurable carbon pool dynamics in long-term incubations. **Soil Biology and Biochemistry**, v. 41, n. 2, p. 357–366, 2009.

VERSINI, A. et al. Nitrogen dynamics within and between decomposing leaves, bark and branches in Eucalyptus planted forests. **Soil Biology and Biochemistry**, v. 101, p. 55–64, 2016.

VON LÜTZOW, M. et al. Stabilization of organic matter in temperate soils: mechanisms and their relevance under different soil conditions - a review. **European Journal of Soil Science**, v. 57, n. 4, p. 426–445, ago. 2006.

XIAO, C. et al. Priming of soil organic matter decomposition scales linearly with microbial biomass response to litter input in steppe vegetation. **Oikos**, v. 124, n. 5, p. 649–657, 2015.

ZECH, W. et al. CPMAS 13C NMR and IR spectra of spruce and pine litter and of the Klason lignin fraction at different stages of decomposition. **Zeitschrift für Pflanzenernährung und Bodenkunde**, v. 150, n. 4, p. 262–265, 1987.